#### Contents lists available at ScienceDirect

# Electrochimica Acta

journal homepage: www.journals.elsevier.com/electrochimica-acta





# Early-stage techno-economic evaluation of electrochemical nitrogen reduction to ammonia based on catalyst performance

Michael J. Rix <sup>a</sup>, Alexander Mitsos <sup>b,a,c</sup>,\*

- <sup>a</sup> Process Systems Engineering (AVT.SVT), RWTH Aachen University, 52074 Aachen, Germany
- b JARA-ENERGY, 52056 Aachen, Germany
- <sup>c</sup> Energy Systems Engineering (ICE-1), Forschungszentrum Jülich, 52425 Jülich, Germany

#### ARTICLE INFO

# Keywords: Nitrogen reduction reaction Power-to-ammonia Techno-economic analysis Catalyst evaluation Performance requirements Performance targets

#### ABSTRACT

The direct electrochemical reduction of nitrogen offers a promising alternative to produce ammonia, an important chemical and potential energy carrier. While current research focuses on developing and improving catalysts for this reaction, studies evaluating the process and establishing catalyst performance targets remain limited. We performed a techno-economic analysis to evaluate the process based on the performance of the nitrogen reduction reaction catalyst. As a result, we identify catalyst performance targets: minimal performance levels as a combination of cell potential, Faraday efficiency, and current density required to reach cost parity with benchmark prices. The minimal catalyst performance levels are illustrated via curves that relate the required current density to the Faraday efficiency. For a competitive process, current densities and Faraday efficiencies above 100 mA cm<sup>-2</sup> and 60%, respectively, are required. Although some catalyst development studies report sufficiently high Faraday efficiencies, the current densities are well below the required. Contrary to the literature's emphasis on maximizing the Faraday efficiency, our results underscore the need for higher current densities at sufficiently high Faraday efficiencies. Although parameters such as electricity or benchmark prices change the absolute values of the required catalyst performance, the primary conclusions remain unchanged. This analysis provides clear guidance for future catalyst development.

# 1. Introduction

Ammonia is a crucial chemical [1,2] and has great potential as a future (sustainable) energy carrier [3]. Today, ammonia is mostly produced via the Haber–Bosch (HB) process from hydrogen and nitrogen [1]. Because hydrogen stems mostly from fossil fuels (steam methane reforming or coal gasification), ammonia production results in high greenhouse gas (GHG) emissions.

Different technologies for reducing GHG emissions in ammonia production are discussed in the literature. Conventional HB plants can be retrofitted with carbon capture units to reduce GHG emissions in hydrogen production [4]. However, retrofitting with carbon capture can result in lower but not zero GHG emissions and does not reduce the dependency on fossil fuels. Electrochemical technologies powered by (renewable) electricity can aid in overcoming this dependency on fossil fuels. Coupling water electrolysis for hydrogen production and HB reduces GHG emissions and the reliance on fossil fuels [3,4]. An emerging technology is the electrochemical nitrogen reduction reaction (NRR). Ammonia is produced in a single electrolyzer using water, nitrogen, and electricity [3–5]. An alternative electrochemical process

is the Li-mediated pathway with lithium nitrate as intermediate [4]. The Li-mediated pathway requires high cell potentials, which decreases energy efficiency [4,6]. All electrochemical processes emit zero GHG emissions during production when powered with renewable electricity and are independent of fossil fuels.

In this work, we focus on evaluating the NRR pathway. A theoretical advantage of the NRR process is its lower minimum energy demand compared to EHB. The equilibrium potential of water electrolysis is higher than that of the NRR reaction [7]. In the HB, first, hydrogen is formed, and then ammonia is synthesized in a highly exothermal reaction. However, the real energy demand of the NRR process is expected to be higher or in a similar range due to higher overpotentials in the electrochemical reaction [4]. Additional benefits of the NRR process include the potential for flexible operation with intermittent electricity sources, the requirement of only one reactor, and the operation at near-ambient pressures and temperatures. Therefore, the NRR process is a promising long-term candidate for (sustainable) ammonia production [4].

<sup>\*</sup> Corresponding author at: Process Systems Engineering (AVT.SVT), RWTH Aachen University, 52074 Aachen, Germany. E-mail address: amitsos@alum.mit.edu (A. Mitsos).

In an NRR electrolyzer as considered here, three reactions take place. At the cathode, ammonia is formed via the NRR and the byproduct hydrogen via the competing hydrogen evolution reaction (HER) [8]. At the anode, oxygen is formed via the oxygen evolution reaction to supply the required protons. While the anode side is similar to water electrolysis, the cathode side requires innovative catalysts to improve the reaction rate and to favor the NRR over the HER to improve the ammonia selectivity, also termed "Faraday efficiency".

Various reviews summarizing the effort in catalyst development are reported in the literature, including [5,7,9–15]. They conclude similar challenges in catalyst and process development. They state the low Faraday efficiency as the main challenge and attribute it to the competing HER and the low catalytic activity of the NRR [5,9,10,14,15]. They give multiple reasons for the low activity. Nitrogen is a stable molecule with a triple bond, resulting in a low reactivity [13]. The low solubility of nitrogen in the aqueous electrolyte and mass transfer resistances reduces the nitrogen availability at the electrode and thus the reactivity [11]. The NRR is kinetically limited compared to the competing HER because six electrons must be transferred in one reaction compared to two [7]. They state these challenges and conclude that considerable catalyst improvement is required, but they do not give concise targets for catalyst development in terms of required catalyst performances.

This gap can be addressed through a techno-economic analysis, which assesses the current state of catalyst development and establishes appropriate catalyst performance targets. Hochman et al. [16] compared the production costs of ammonia across different technologies. They evaluated the NRR process assuming a high Faraday efficiency of 95% and a low cell potential, which results in a low energy demand. Moreover, they directly transferred investment cost from water electrolysis based on the cost per unit of current thus implying a similar reaction rate in the NRR as in water electrolysis. With these optimistic assumptions, the NRR process can be competitive with EHB. Fernandez and Hatzell [17] compared ammonia production via NRR with water electrolysis followed by electrochemical ammonia synthesis from hydrogen and nitrogen. They estimate investment costs by transferring projected costs for mass-produced automotive PEM fuel cells, resulting in low investment costs. A sensitivity analysis on various parameters indicated that investment costs have a minimal impact due to their already low initial values. By varying the design and performance parameters, they demonstrated that both approaches could compete with the HB process on a small scale due to the assumed low investment cost of the NRR process versus the higher investment cost of small-scale HB. Additionally, they calculated the feasible space in current density and Faraday efficiency to achieve cost parity with large-scale and small-scale ammonia production under their assumptions. Wang et al. [18] also evaluated ammonia production technologies by assuming values for reactivity, selectivity, and energy demand. Based on their assumptions, all processes resulted in similar production cost ranges, with NRR yielding the lowest.

The studies cited above investigated the ammonia production cost based on assumptions on the process performance. They assumed catalyst performances, leading to overly favorable techno-economic outcomes. None of the studies put their assumptions regarding the catalyst performance into perspective to the performances achieved in the literature. Further, they do not address the low TRL and possible scalability limitations. They calculated investment costs by directly transferring water electrolysis costs irrespective of differing reaction rates and system components. These limitations result in overly favorable technoeconomic outcomes which do not align with the current state of the process.

In the literature, cost calculations are conducted for different electrochemical systems at low TRL. Kim et al. [19] estimated the investment cost of anion exchange membrane water electrolysis (AEM) from

PEM water electrolysis by keeping the system cost constant and replacing the stack components. They scaled the PEM stack costs to AEM using material cost factors, assuming a similar set-up using different materials. In their study on electrochemical co-production, Na et al. [20] transferred PEM cost scaled with the applied catalysts. Moreno-Gonzalez et al. [21] estimated the investment cost of electrochemical CO<sub>2</sub> reduction by transferring cost from water electrolysis, exchanging cost for the electrodes, and adding cost for the GDE. Other works such as [22–24] directly transferred cost data from water electrolysis without accounting for differences in technologies. We calculated investment costs by extending the method from Moreno-Gonzalez et al. [21] by transferring the water electrolysis cost and exchanging and adding the required stack and system components.

The contribution of this work is to establish appropriate performance targets for NRR catalyst development to achieve cost parity with conventional and green ammonia production technologies. To do so, we investigated the influence of the NRR catalyst performance on both process efficiency and economics. We conducted a technoeconomic study for a mid-site NRR process (nominal power of 100 MW) based on the performance characteristics of the NRR catalyst. Unlike previous techno-economic studies, which focused on specific operating points with defined catalyst performance, we calculated the required catalyst performance to achieve cost parity with benchmark prices. This approach allowed us to identify the feasible space for an economically viable process and to set clear performance targets for catalyst development. We investigated the catalyst performance parameters cell potential, Faraday efficiency, and current density. Building on this analysis, we critically reviewed the current state of catalyst development to put it into perspective by evaluating the performance improvement required to reach cost parity with benchmark prices. Through this methodology, we showed that multiple combinations of catalyst performance parameters can yield an equivalent process performance. Suitable performance targets for catalyst development are not one operating point but a feasible parameter space.

Process modeling and techno-economic analyses at low TRL are established tools for assessing a technology's current state and guiding R&D. Exemplarily, Mitsos et al. [25] assessed how catalysts should be improved in man-portable power generation devices. Jouny et al. [26] derived performance targets for the cell voltage and Faraday efficiency for  $\rm CO_2$  electrolysis to different products at a defined current density, and Cruellas et al. [27] identified yield targets for oxidative methane coupling.

The rest of the article is structured as follows. In Section 2, we introduce the NRR process. Section 3 details the process model and the calculation of the minimal catalyst performance levels. In Section 4, we present these minimal catalyst performance levels and compare them to the catalyst performance achieved in the literature. We discuss the results and evaluate the improvements required for the NRR process in Section 5 and conclude the key findings and future work in Section 6.

#### 2. Process description

We divide the NRR process into three stages: (i) upstream supply of the reactants, (ii) ammonia production in the electrolyzer, and (iii) downstream separation of ammonia, see Fig. 1. Nitrogen is supplied from an air separation unit, and de-ionized water is obtained from water desalination. The electrolyzer is the core component of this process where nitrogen and water are converted to ammonia by consuming electrical energy. Downstream, ammonia is separated and purified from the unreacted reactants, the electrolyte, and by-products.

This subdivision into the three stages allows us to focus on the electrolyzer while disregarding the up- and downstream processes. This simplifies the analysis because the design and operation of up- and downstream processes depend on the catalyst performance and the operating conditions, which are unknown at the time of this investigation. By focusing on the electrolyzer and disregarding the up- and

Fig. 1. Block diagram of the NRR process. Solid black lines represent material flow, dashed red lines electricity flow, and dotted blue lines heat flow.

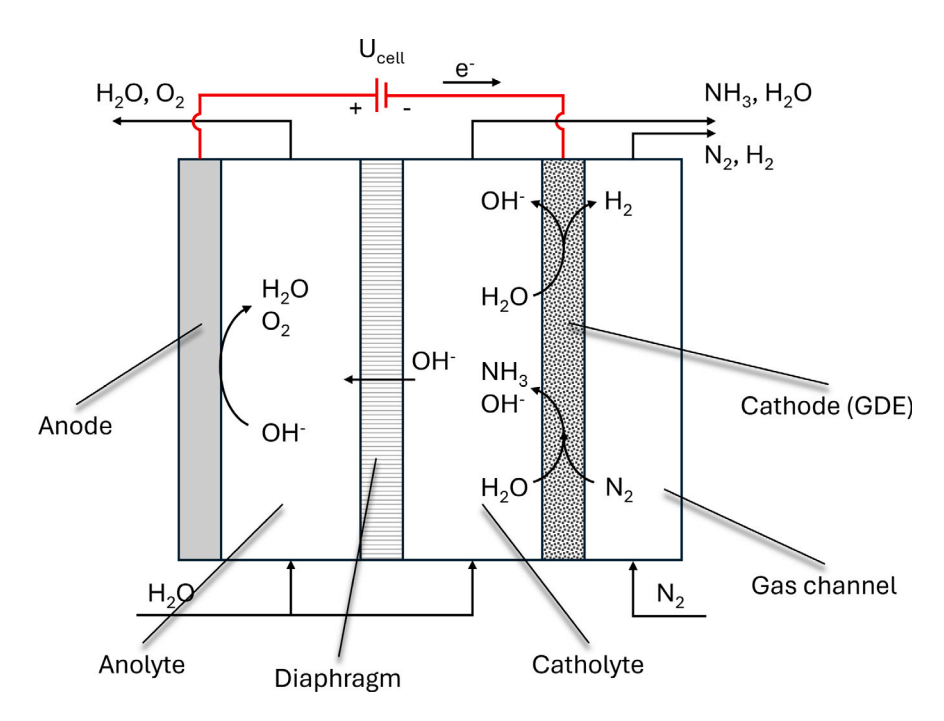


Fig. 2. Sketch of an electrolyzer for the NRR process in alkaline conditions with a GDE as a cathode. Black lines represent material flow and red lines electricity flow. We assume that only hydroxide ions diffuse through the diaphragm.

downstream processes, we overestimate overall process performance and thus underestimate the *minimal electrolyzer performance* required for benchmark parity. A catalyst for a real process must perform better than the performance requirements derived in this work. However, the derived minimal performance yields a lower bound for catalyst development and is useful for putting recent progress into perspective to the minimal required performance.

The catalyst has a direct impact on the electrolyzer while up- and downstream processes are similar for all catalysts. The separation effort depends on the concentration of ammonia in the product stream, which itself depends on the operating conditions and the catalyst performance but not on the catalyst material. Similarly, the reactant demand will be independent of the catalyst material.

Process intensification methods, such as heat integration, can improve the overall efficiency of electrochemical plants by utilizing excess heat from the electrolyzer to reduce the energy demand of up-and downstream processes (e.g., [28,29]). In the NRR process, the electrolyzer requires electricity and releases heat while the up- and downstream processes also require electricity and may require or release heat. Since no sub-process generates electricity, the electrolyzer efficiency cannot be improved by process intensification, and up- and downstream processes can only reduce the overall efficiency. The electricity demand of the process can only be similar or higher when considering up- and downstream processes, not lower.

Different electrolyzer concepts for the NRR process exist. The reaction can take place in alkaline, neutral, or acidic conditions [8].

Nitrogen is supplied with a gas diffusion electrode (GDE) to achieve a higher nitrogen availability at the electrode for enabling high reaction rates. Either a zero-gap or finite-gap membrane electrode assembly can be applied. Fig. 2 shows the layout of a finite gap electrochemical cell with a GDE for alkaline conditions as considered in this evaluation. The detailed electrolyzer concept or setup does not play a role at the considered level of detail and does not influence this evaluation because the main components are similar.

At the cathode, the NRR reaction forming ammonia takes place. In a competing reaction, hydrogen is formed in the hydrogen evolution reaction (HER). The HER is the only side reaction considered in this work. Experimental investigations showed that the generation of further by-products such as hydrazine is negligible [13,30–32]. In alkaline conditions, the overall half-cell reactions of the NRR and HER are:

NRR: 
$$N_2 + 6 H_2 O + 6 e^- \rightleftharpoons 2 NH_3 + 6 OH^ E^0 = -0.739 V$$
  
HER:  $2 H_2 O + 2 e^- \rightleftharpoons H_2 + 2 OH^ E^0 = -0.828 V$ 

At the anode, oxygen is formed in the oxygen evolution reaction (OER)

$$2 H_2 O + O_2 + 4 e^- \longrightarrow 4 O H^ E^0 = 0.401 \text{ }^{-1}$$

by oxidizing hydroxide ions to water and oxygen and releasing electrons.

Commercial catalysts from water electrolysis exist for the anode. For the cathode, novel catalysts favoring the NRR are required. Thus, the performance of the process will be determined by the NRR catalyst at the cathode. A promising NRR catalyst has a high selectivity towards ammonia at high current densities and low cell potentials.

How a catalyst can be improved for the NRR is discussed elsewhere in detail, e.g., [11,13]. The Faraday efficiency can be improved by favoring nitrogen activation. By reducing the NRR overpotential, either the cell voltage can be reduced at a certain current density or the current density can be increased at a certain cell voltage.

#### 3. Process model

We evaluate the influence of NRR catalyst performance on the overall process performance. In the following, we derive a model to estimate the energy demand and the required electrolyzer size for producing a certain amount of ammonia for an electrolyzer comparable to Fig. 2. The model estimates the ammonia production cost based on the catalyst performance, specifically the achieved Faradaic efficiency at a certain current density and cell potential. Both investment (CAPEX) and operating cost (OPEX) are estimated to evaluate the total production cost.

As stated above, we focus on evaluating the electrolyzer and neglect the up- and downstream processes. In deriving the electrolyzer model and cost calculation, we assume

- · a continuous operation
- a plant lifetime of 10 years with 8,000 h of operation per year
- constant prices for electricity and ammonia over the whole plant lifetime
- · zero cost for reactants
- · an electrolyzer nominal power of 100 MW (mid-scale process)
- a uniform concentration along the electrode (lumped model, i.e., 0D)
- that mass transport overpotentials are included in the cell potential
- that the HER is the only side reaction
- · that no shunt currents or other current losses occur
- a direct comparability between literature data and the calculated minimal performance

In Section 3.1 we introduce the process model for the electrolyzer. In Section 3.2 we explain the cost calculation for this novel process. Combining these, we derive the relationship between the production cost and the catalyst performance (i.e., the cell potential, current density, and Faraday efficiency) in Section 3.3.

# 3.1. NRR electrolyzer model

As aforementioned, the electrolyzer is modeled to calculate the ammonia production rate, the specific energy demand of ammonia production, and the electrolyzer size. The ammonia production rate is calculated with Faraday's law as

$$\dot{m}_{\rm NH3} = \frac{\dot{j}_{\rm NH3} A_{\rm Elec} M_{\rm NH3}}{\tau^E} \tag{1}$$

with the ammonia current density  $j_{\rm NH3}$  (current going into the NRR), the total electrode surface area  $A_{\rm Elec}$ , the molar mass of ammonia  $M_{\rm NH3}$ , the number of electrons transferred to produce one molecule of ammonia z, and Faraday's constant F. The yearly production of ammonia is the production rate times the yearly operating hours  $t_{\rm op}$ ,

$$m_{\rm NH3} = \dot{m}_{\rm NH3} \cdot t_{\rm op}. \tag{2}$$

The specific energy demand  $p_{\rm El}$  of the electrolyzer is calculated using

$$p_{\rm El} = \frac{P_{\rm El}}{\dot{m}_{\rm NH3}} = \frac{j_{\rm tot} A_{\rm Elec} U_{\rm cell}}{\dot{m}_{\rm NH3}}. \label{eq:pel}$$

depending on the cell potential  $U_{\rm cell}$ , the total current density  $j_{\rm tot}$ , the electrolyzer area  $A_{\rm Elec}$ , and the ammonia production rate  $\dot{m}_{\rm NH3}$ .

The current density is a measure of the reaction rate; higher current densities reflect higher reaction rates. With the Faraday efficiency  $\eta_{FF}$ ,

$$\eta_{\text{FE}} = \frac{j_{\text{NH3}}}{j_{\text{tot}}},$$

a dependency between the ammonia current density and the total current density is introduced. The Faraday efficiency describes the share of current (density) for ammonia production. The remaining current ( $(1-\eta_{\rm FE})\cdot j_{\rm tot}$ ) is the current for hydrogen production from the side reaction and shunt currents. Shunt currents are current losses in real-world systems, e.g., due to the diffusion of products through the membrane or bypass currents following paths different from the electrochemical reactions [33]. The magnitude of shunt currents depends on the electrolyzer setup and operating conditions and is not known at the current state of development. In our analyses—except for when the by-product hydrogen is sold—all current not going into ammonia synthesis is considered a current loss, and therefore distinguishing between HER and shunt current losses can be ignored.

We do not consider the formation of other by-products such as hydrazine. Experimental studies showed that the formation of these by-products is negligible [13,30–32]. This might change with deviating operating conditions. However, this cannot be investigated without reliable experimental evidence. Thus, we ignore the formation of further by-products. Again, this is only of importance when the by-product hydrogen is sold. Otherwise, all current losses are considered together.

Concluding, the specific energy demand can be calculated as

$$p_{\rm El} = \frac{zF}{M_{\rm NH3}} \frac{U_{\rm cell}}{\eta_{\rm FE}}.$$
 (3)

The Faraday efficiency determines the number of electrons required to produce a certain amount of ammonia; the cell potential determines the energy required to transfer these electrons. The cell potential depends on the equilibrium potentials of the half-cell reactions and various overpotentials such as the activation overpotential of the NRR. As these potentials can vary depending on the operating conditions, the electrolyzer set-up, the current density, and the catalysts, we do not calculate them explicitly. We investigate the influence of the cell potential as a catalyst performance parameter by varying it in a reasonable interval. Thus, we can independently study the effect of cell potential and current density.

We assume the cell potential to be constant over the lifetime of the plant and ignore variations in the overpotentials caused by catalyst degradation or temperature effects. Long-term experimental studies in pilot plants are required to capture these effects. Thus, the cell voltage can be understood as a mean value over the plant's lifetime.

The electrolyzer model is 0D, i.e., we assume a uniform concentration along the electrode. This idealization gives the highest reaction rate possible and thus overestimates productivity. This overestimation yields an underestimation of the required catalyst performance. Thus, we identify *minimal* catalyst performance targets.

# 3.2. Levelized cost of ammonia

We calculate the levelized cost of ammonia LCOA depending on the catalyst performance to compare it with certain benchmark prices. The LCOA is the price at which ammonia must be sold such that the net present value at the end of the plant lifetime (usually 10 or 20 years) is zero. The LCOA is defined as

$$LCOA = \frac{CRF \cdot CAPEX + OPEX_{O\&M} + OPEX_{El}}{m_{NH3}}$$
 (4)

with the investment cost CAPEX, the cost of operation and maintenance OPEX $_{\rm O\&M}$ , the electricity cost OPEX $_{\rm El}$ , and the yearly produced amount of ammonia  $m_{\rm NH3}$ . The capital recovery factor CRF

CRF = 
$$\frac{i(1+i)^N}{(1+i)^N - 1}$$

is used to calculate the annualized cash flow from the initial investment depending on the length of the investment period N and the interest rate i.

M.J. Rix and A. Mitsos Electrochimica Acta 523 (2025) 145893

#### 3.2.1. Operating cost calculation

The electricity cost  $OPEX_{El}$  is calculated depending on the specific energy demand  $p_{El}$ , the yearly ammonia production rate  $m_{NH3}$  and the electricity price  $c_{El}$  using

$$OPEX_{El} = p_{El} \cdot m_{NH3} \cdot c_{El}$$
.

Inserting Eq. (3) yields the electricity cost depending on the cell potential and Faraday efficiency:

$$OPEX_{El} = \frac{zF}{M_{NH3}} \frac{U_{cell}}{\eta_{FE}} \cdot m_{NH3} \cdot c_{El}.$$
 (5)

The operation and maintenance cost is calculated as a fraction of the investment cost,

$$OPEX_{O\&M} = f_{O\&M} \cdot CAPEX,$$

with the factor  $f_{\text{O\&M}}$  accounting for operation, maintenance, and insurance [34].

#### 3.2.2. Capital investment cost estimation

In the absence of more accurate data, we estimate capital investment costs by transferring results from water electrolysis cost studies while considering technological differences. We follow a methodology similar to Moreno-Gonzalez et al. [21], who accounted for differences in the electrode material and assembly as well as costs associated with a GDE. We extend this methodology by not only accounting for a GDE but also for differing reaction rates and sizes of stack and system in the NRR and water electrolyzer.

There are various studies on capital investment cost calculation of water electrolysis in the literature. IRENA [35] identifies two main challenges in investment cost calculation of water electrolysis: (i) the availability of data and (ii) inconsistent boundaries in cost estimate studies (e.g. stack, system, or full plant). The results will depend on the selected reference study. We use the cost analysis by Holst et al. [36] as a reference study. They performed a bottom-up cost analysis of PEM and alkaline water electrolysis starting at the material level of the stack components and going up to the system level. They studied two different plant sizes (5 MW and 100 MW). Following this bottom-up approach, the system boundaries are defined and data for all components at all system scales is available. All relevant information for transferring the cost of the required components is available.

We use the cost of the alkaline water electrolyzer plant because this set-up is most similar to the NRR set-up (compare Fig. 2) for a nominal power of  $100\,\mathrm{MW}$ . The reported cost breakdown is given in in the supplementary information (SI) in Table S.5. Holst et al. [36] report the cost data in  $\mathrm{CkW}^{-1}$ . Thus, everything is scaled according to the electrolyzer's nominal power. However, not everything will scale according to the nominal power when transferring to a different reaction system. A plant with the same nominal power but half the nominal current density will require similar power electronics but twice the electrolyzer cell area. Power electronic costs will be similar but cell and stack costs will be higher, which needs to be accounted for in the cost calculation.

When transferring the cost to the NRR case, we distinguish between components scaling with the nominal power and components scaling with the cell area. Components such as power electronics, balance of plant, or cooling are mainly determined by the nominal power and are scaled accordingly. Components such as the stack number, piping, or housing are determined by the required cell area and are scaled accordingly. For the components scaling with the electrolyzer area, we calculate the area-dependent cost (in  $\mathbb{C}\,\mathrm{m}^{-2}$ ) by multiplication with the nominal power density considered in the reference cost analysis [36]. Table S.5 shows which component is scaled according to which variable. Following this, the investment cost CAPEX can be calculated as

$$CAPEX = c_A \cdot A_{Elec} + c_P \cdot P_{Elec}$$
 (6)

Table 1
Cost factors for investment cost calculation

Good factors for investment cost careanation.		
$c_A$	4298.9	€ m <sup>-2</sup>
$c_P$	240.5	€ kW <sup>-1</sup>

with the area- and power-dependent cost factors  $c_A$  and  $c_P$ , respectively, and the electrolyzer area  $A_{\rm Elec}$ , and the nominal power  $P_{\rm Elec}$ .

The area-dependent cost also includes a cost factor for the GDE of  $60 \text{ m}^{-2}$  [21]. With this and the data from Table S.5, the cost factors conclude to Table 1.

This method allows us to estimate the capital investment costs for the NRR process while taking into account technology differences in terms of the required electrolyzer components and reaction rates. This approach is as thorough as possible and uses all available data. However, if the NRR catalyst is considerably more expensive or if additional components not considered here are required, the investment cost may be underestimated. When analyzing a specific catalyst, accurate catalyst costs or any additional components can be incorporated into the cost calculation.

#### 3.3. Cost calculation based on catalyst performance

To recall, our goal is to calculate the ammonia production cost based on the performance of the cathode-side catalyst. At the cathode, the NRR takes place and ammonia is synthesized. We calculate the required catalyst performance to achieve ammonia production cost parity with different benchmark prices to assess the current state and potential progress and to derive future performance targets for experimental catalyst development.

The catalyst performance is evaluated based on the Faraday efficiency, cell potential, and current density—parameters commonly reported in catalyst studies. Although these parameters are physically interdependent, we evaluate them separately to define a feasible parameter space for economically viable catalysts in all three parameters. This feasible parameter space establishes the minimum performance requirements for NRR catalysts, thereby serving as a target for developing economically viable catalysts. Additionally, this framework can be used to compare reported catalysts and to put them into perspective to requirements for an economically viable process.

For a certain production rate, the current density multiplied by the Faraday efficiency directly determines the required electrolyzer area Eq. (1) and thus the area-dependent investment cost Eq. (6). The cell potential and Faraday efficiency determine the power demand Eq. (3) and thus the electricity cost Eq. (5) and the power-dependent investment cost Eq. (6). The LCOA Eq. (4) results to

$$\begin{split} \text{LCOA} &= \frac{zF}{M} \cdot \frac{1}{\eta_{\text{FE}}} \cdot \left( \frac{(\text{CRF} + f_{\text{O\&M}})}{t_{\text{op}}} \cdot \frac{1}{j_{\text{tot}}} \cdot c_A \right. \\ &+ \left. \left( \frac{(\text{CRF} + f_{\text{O\&M}})}{t_{\text{op}}} \cdot c_P + c_{\text{El}} \right) \cdot U_{\text{cell}} \right) \end{split} \tag{7}$$

depending on the catalyst parameter Faraday efficiency  $\eta_{\rm FE}$ , current density  $j_{\rm tot}$ , and cell voltage  $U_{\rm cell}$ . It is obvious that the Faraday efficiency and current density should be as high as possible and the cell voltage as low as possible. However, these parameters are interdependent and it is unknown how well the catalyst must perform.

To determine how well the catalyst must perform, we calculate the catalyst performance required to reach cost parity with a certain benchmark rather than evaluating Eq. (7) for a certain catalyst. We set the LCOA Eq. (7) to a benchmark price  $c_B$ ; reformulation yields Eq. (8) to calculate the required current density at a given cell potential and Faraday efficiency:

$$j_{\text{tot}} = \frac{(\text{CRF} + f_{\text{O\&M}}) \cdot c_A \cdot \frac{zF}{M} \cdot \frac{1}{t_{\text{op}}}}{\eta_{\text{FE}} \cdot c_B - \left[ (\text{CRF} + f_{\text{O\&M}}) \cdot \frac{1}{t_{\text{op}}} \cdot c_P + c_{\text{El}} \right] \cdot \frac{zF}{M} \cdot U_{\text{cell}}}.$$
 (8)

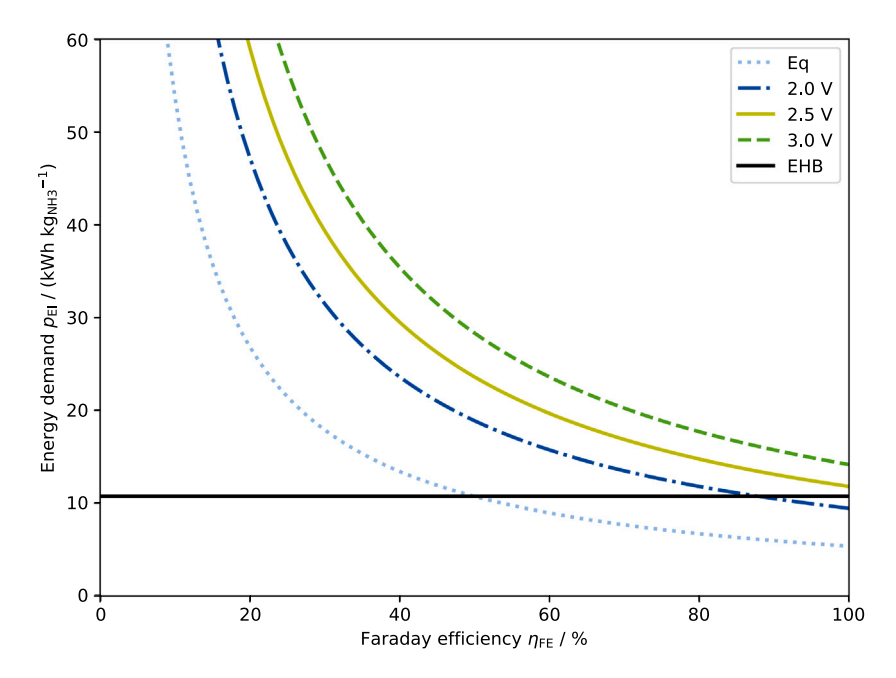


Fig. 3. Energy demand of NRR ammonia production at different cell potentials. The black curve shows the energy demand of ammonia production via water electrolysis and EHB [37,38].

We calculate the required catalyst performance in terms of the required current density  $j_{\rm tot}$  at a certain Faraday efficiency  $\eta_{\rm FE}$  and cell potential  $U_{\rm cell}$ . The parameter values used in the evaluation are given in the SI in Table S.6.

We compare the production cost of ammonia with the market price and projected values for green ammonia via the EHB process. Benchmarking green ammonia against fossil-based ammonia sets an unrealistically high standard, as the hydrogen source in HB is typically inexpensive coal or natural gas, both energy-dense fossil resources. Utilizing these sources leads to significant GHG emissions, which are not reflected in the cost calculations. Both EHB and NRR processes use water as a hydrogen source, requiring considerable electricity input. A comprehensive comparison between sustainable and fossil-based production must take GHG emission costs into account; however, this falls outside the scope of our work and would involve policy discussions. To overcome this, we compare NRR production cost with the current ammonia market price, which includes the current policies, and with projected green ammonia costs, which include the current policies in the electricity price. Future policies will similarly influence EHB and NRR and, therefore, they will not significantly impact the comparison between the two technologies.

We ignore market dynamics such as fluctuations in electricity prices, ammonia prices, and feedstock availability. These market dynamics are out of the scope of this analysis. Further, they will have a similar impact on the NRR technology and the EHB benchmark and thus limited influence on the required catalyst performance.

#### 4. Results and discussion

First, we present results on the energy demand of the NRR process and compare it with the EHB process in section Section 4.1. Second, we calculate the required catalyst performance for cost parity and compare it with catalyst data reported in the literature in Section 4.2. Finally, we perform a sensitivity analysis on assumed cost parameters, the influence of catalyst replacement, and estimate how selling the by-product hydrogen can affect process economics in Section 4.3.

#### 4.1. Energy demand of electrochemical ammonia production

We calculate the specific energy demand of NRR ammonia production with Eq. (3) as a function of the cell potential and the Faraday efficiency. As stated above, the current density does not influence the energy demand in this analysis because the cell potential is investigated as a performance parameter and we do not investigate the influence of the current density on the potential itself. We compare the specific energy demand with the EHB process which is expected to be in the range of  $10.5\,\mathrm{kWh}\,\mathrm{kg}_\mathrm{NH3}^{-1}$  to  $11\,\mathrm{kWh}\,\mathrm{kg}_\mathrm{NH3}^{-1}$  [37,38].

Fig. 3 shows the NRR energy demand plotted against the Faraday efficiency, the curves refer to constant cell potentials. The NRR energy demand is evaluated at four cell potentials: at equilibrium conditions (minimum energy demand) and between 2 V to 3 V, with the highest being the upper limit for the expected cell potential at industrial conditions [39]. The black line shows the EHB energy demand as a reference (which is independent of the Faraday efficiency).

Eq. (3) shows that the energy demand scales linearly with the cell voltage and inversely with the Faraday efficiency  $(1/\eta_{FE})$ . Thus, the NRR energy demand decreases with increasing Faraday efficiency and decreasing cell potential. The decrease in energy demand is steep at low Faraday efficiencies and eases out with higher. This shows that increasing the Faraday efficiency particularly influences the energy demand at low Faraday efficiencies. At higher Faraday efficiencies, less by-product is formed and a higher share of the electricity is used to produce the desired product.

An energy-efficient catalyst yields a high Faraday efficiency at low cell voltages. The influence of the catalyst on the cell voltage is limited. The catalyst only influences the NRR activation overpotential; the equilibrium potential and losses such as the anodic overpotential and ohmic losses cannot be reduced by catalyst development. The Faraday efficiency is determined by the catalyst and electrolyzer setup [11,13] and can be increased by catalyst development.

Comparing the NRR and EHB energy demand shows that the NRR's energy demand is lower at cell potentials close to equilibrium and high Faraday efficiencies. At the equilibrium potential—the thermodynamic minimum at standard conditions—the energy demand is lower even at Faraday efficiencies below 60%. This shows the theoretically lower energy demand and potential of the NRR process. In contrast, at a cell

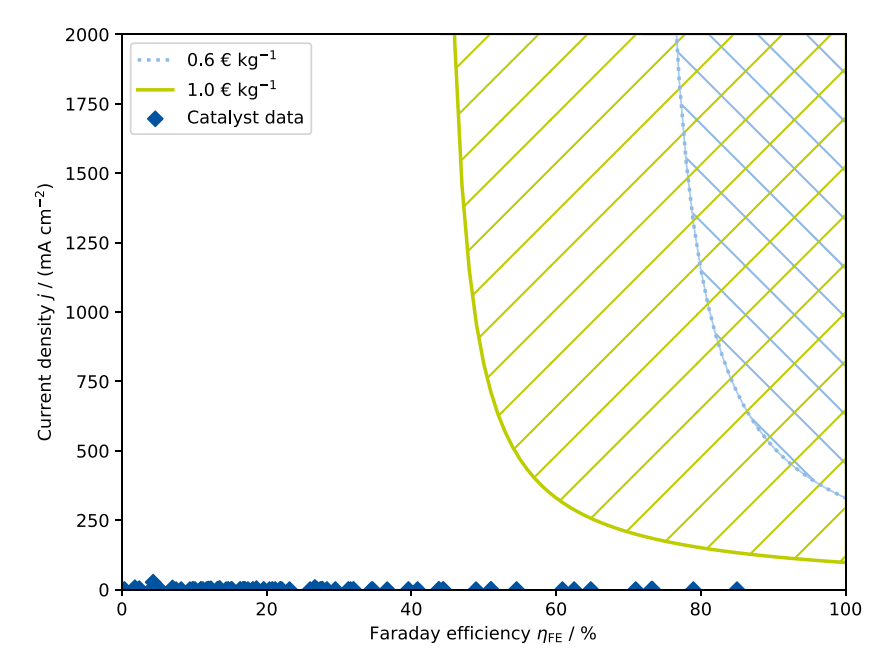


Fig. 4. Comparison of catalyst data reported in the literature (blue diamonds) and calculated cost parity curves. The blue curve shows the required current density to reach cost parity against the Faraday efficiency for a benchmark price of  $c_B = 0.6 \, \text{kg}_{\text{NH3}}^{-1}$ , the green curve for a benchmark price of  $c_B = 1 \, \text{kg}_{\text{NH3}}^{-1}$ . Both curves are calculated assuming a constant cell potential of 2.5 V and an electricity price of  $30 \, \text{e}$  MWh<sup>-1</sup>. For an economically viable process, a catalyst must lie in the shaded regions on or above the curves.

potential of  $U_{\rm cell}=2.0\,{\rm V}$  the NRR's energy demand is higher for all Faraday efficiencies lower than 90% and at a cell potential of 2.5 V it is higher for all Faraday efficiencies.

Despite the theoretically lower energy demand, the actual feasible space with a lower energy demand is small. Because the equilibrium voltage of NRR—the minimum energy demand—is only  $0.089\,\mathrm{V}$  lower than that of water electrolysis, both water electrolysis and NRR will operate at similar cell voltages. Water electrolysis accounts for more than 90% of the energy demand in EHB. Therefore, there is a limited potential for the NRR technology from an energetic point of view. Faraday efficiencies lower than 90% and cell voltages above  $2\,\mathrm{V}$  will result in a higher energy demand of the NRR.

The EHB process requires upstream processes for providing pure water and nitrogen, water electrolysis to produce hydrogen, compression of hydrogen and nitrogen to reaction pressure, a two- or three-bed reactor for ammonia production, and an ammonia separation process. The NRR process requires similar upstream processes, ammonia electrolysis, and ammonia separation (Fig. 1). Thus, the EHB process requires considerably more equipment compared to the NRR process. The NRR is a one-step reaction, promising a process intensification and consequently lower investment costs compared to the two-step EHB process. In the following, we calculate production costs and derive the NRR catalyst performance required to achieve cost parity with conventional and green ammonia benchmarks.

#### 4.2. Catalyst performance required to reach production cost parity

We conduct an economic analysis to investigate the process economics depending on the catalyst performance—specifically, Faraday efficiency, current density, and cell potential. Using Eq. (8), we calculate the catalyst performance required to achieve cost parity with a benchmark price. We assume a mid-size process with a nominal power of 100 MW as a reference for the cost calculation. We vary the cell potential and Faraday efficiency to calculate the current density required for cost parity. This approach allows us to identify the feasible space for catalyst development for economically viable processes. We then compare these findings with catalyst data reported in the literature to assess the current state of the process and to define realistic performance targets for catalyst development.

Fig. 4 compares the cost parity curves for a benchmark price of  $0.6 \, \&\, kg_{NH3}^{-1}$  (blue curve, assumed market price) and  $1.0 \, \&\, kg_{NH3}^{-1}$  (green curve, expected green ammonia price) with catalyst data reported in the literature (dark blue diamonds, [40–125], collected and assigned as probably reliable results by [5], data given in the SI in Table S.7). The curves show the required current density,  $j_{tot}$ , at a certain Faraday efficiency to reach cost parity for a cell potential of 2.5 V (assumed to be constant). A catalyst for an economically viable process must lie in the shaded region on or above the curves. Thus, different combinations of Faraday efficiency and current density are possible and result in the same production cost.

The curves for the two benchmarks have an elbow shape, similar (but steeper) to the energy demand curves (Fig. 3). An economically viable process is not feasible below a minimal Faraday efficiency for both curves. Below this threshold, electricity costs are higher than the benchmark price. Above the minimal Faraday efficiency, the required current density reduces considerably until reaching the elbow point. Beyond this point, the required current density reduces only slightly until reaching the minimal current density at the highest Faraday efficiency (100%). The blue curve representing the lower benchmark price has been shifted to the upper right corner, making the gradual decline after the elbow less visible.

The feasible region for cost parity with the ammonia market price (blue curve) is small; high current densities and Faraday efficiencies must be achieved. For a given Faraday efficiency and cell potential, the power demand and thus the electricity cost and the power-dependent investment cost have a fixed value. The area-dependent investment cost is the only degree of freedom to achieve cost parity. It is calculated as the difference between benchmark price and power-dependent costs. Figure S.1 in th SI shows the evolution of the cost composition over the Faraday efficiency for the higher benchmark price and a more in-depth cost analysis is given in the SI in Section S.3. The power-dependent costs are higher than the benchmark price for low Faraday efficiency, resulting in a negative calculated area-dependent investment cost and thus a negative required current density, which is infeasible.

A higher benchmark price (green curve) does not change the powerdependent cost since the energy demand is the same. However, the difference between the benchmark and the power-dependent cost and

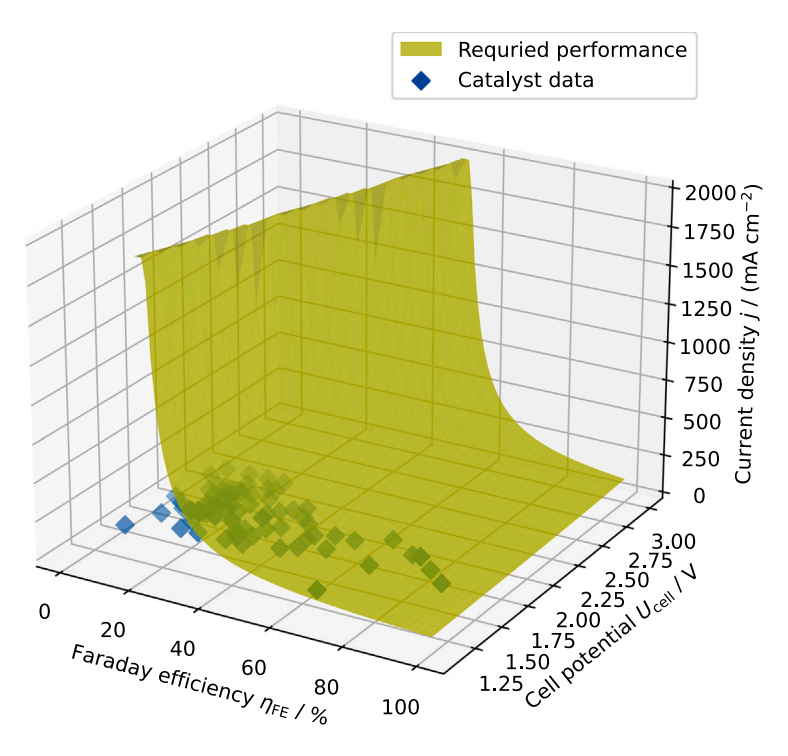


Fig. 5. Influence of the cell potential and Faraday efficiency on the cost parity curves for a benchmark price of  $c_B = 1.0 \, \mathrm{kg_{NH3}^{-1}}$  and an electricity price of  $30 \, \mathrm{cMWh^{-1}}$ . The blue diamonds show reported catalyst data.

thus the area-dependent investment cost increases. Therefore, the area-dependent investment cost becomes positive at lower Faraday efficiency, increasing the feasible space for catalyst performance (Fig. 4).

The reported catalyst performances are well below the cost parity curves for both benchmarks. While the analysis shows that some studies achieve sufficiently high Faraday efficiencies to compete with the green ammonia benchmark, considerable improvements in the current density are crucial. The magnitude of the difference in the achieved and required current density is visualized by plotting the cost parity curves alongside the catalyst data on a logarithmic *y*-axis (see Figure S.2 in the SI). Achieved current densities at relevant Faraday efficiencies are at least two to three orders of magnitude too low, highlighting the considerable challenges still facing catalyst development.

Achieving cost parity with the green ammonia benchmark appears more feasible than with the market price, as the viable region is considerably larger. The required current densities at intermediate to high Faraday efficiencies are lower than those found in industrially relevant processes, such as alkaline water electrolysis, demonstrating the theoretical potential for reaching cost parity.

The third catalyst performance parameter, the cell potential, was set to a constant value. Varying both the Faraday efficiency and the cell potential allows us to compare their influence on the required current density. Fig. 5 shows a 3D plot of the required current density as a function of cell potential and Faraday efficiency compared with reported catalyst performance data. The cell potential data from catalyst studies was reported by Rezaie et al. [5] by adding the expected anode potential to the cathode potentials reported in catalyst studies.

The shape of the required current density surface is similar to the curves in Fig. 4. Increasing the Faraday efficiency beyond the minimal results in a sharp decrease in the required current density followed by a small decrease at high Faraday efficiencies. At a constant Faraday efficiency, reducing the cell potential reduces the required current density. This effect is more prominent at low Faraday efficiencies. At the equilibrium potential, the thermodynamic minimum voltage, the minimal Faraday efficiency is 25%; at the highest expected industrial

cell potential, the minimal Faraday efficiency is 60%. Above Faraday efficiencies of 70% to 80%, the cell potential has little influence on both the production cost and the required current density.

The cell potential is an important catalyst performance parameter at low and intermediate Faraday efficiencies. Here, the production costs are primarily driven by the electricity costs. The cell potential, and consequently the electricity demand, directly influence production costs and the required current density. However, at higher Faraday efficiencies, this influence diminishes.

Cost parity can be achieved for all investigated cell potentials. In contrast, cost parity is not feasible at low Faraday efficiencies or current densities. This shows that both the Faraday efficiency and the current density have a more significant impact on the production cost than maintaining a low cell potential. Achieving high current densities or Faraday efficiencies is more crucial than keeping the cell potential low.

Comparison with experimental data leads to similar conclusions to Fig. 4. The reported catalyst data is outside the feasible region: while some studies achieve sufficiently high Faraday efficiencies, the current densities are too low in all studies. Further, all studies operate at low cell potentials, the highest cell potential is at 2.3 V. The findings above show that operating at higher cell potentials will be beneficial if it results in higher Faraday efficiencies and/or current densities.

Despite the recent progress, the achieved catalyst performance is too low for the NRR process to be competitive with the ammonia market price or green ammonia. Comparing the cost parity curves with the reported catalyst performance shows that improving the Faraday efficiency alone will be insufficient. Catalyst development research should not focus solely on improving the Faraday efficiency but rather shift towards achieving higher current densities while retaining sufficiently high Faraday efficiencies. The current density and Faraday efficiency have a stronger influence on the production cost than the cell potential. While the catalyst's influence on the cell voltage is limited to the NRR activation overpotential, catalyst development and electrochemical engineering can improve both the current density and Faraday efficiency.

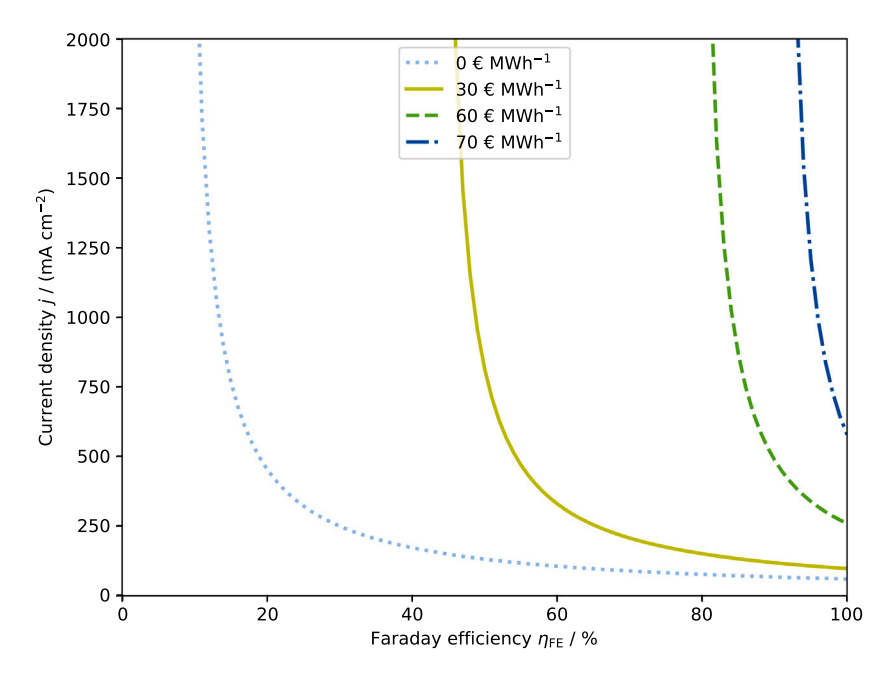


Fig. 6. Influence of the electricity price on the cost parity curves for a benchmark price of  $c_B = 1.0 \, \text{k} \, \text{g}_{NH3}^{-1}$  and a cell potential of 2.5 V.

#### 4.3. Sensitivity analysis on the required catalyst performance

The analysis showed that considerable improvements in the current density are required for an economically viable process. Further, it showed the influence of the ammonia benchmark price on the feasible space for catalyst development. To further quantify the meaningfulness of the results we perform a sensitivity analysis on the cost parameters, the influence of catalyst replacement, and whether the by-product hydrogen can be sold.

#### 4.3.1. Parameter influence

Some parameters in Eq. (8) are uncertain and can influence the process economics. The electricity price depends on the location and future developments in policy and RE implementations. The capital investment cost parameters depend on future technology developments and are unknown due to the low TRL. We evaluate the parameter influence by varying one parameter at a time. The green curve in Fig. 4 for cost parity with EHB for a cell potential of 2.5 V and electricity cost of  $30 \, \epsilon \, \mathrm{MWh}^{-1}$  is the baseline.

Fig. 6 shows the influence of the electricity price on the required catalyst performance. The energy demand analysis (Section 4.1) already showed the strong influence of Faraday efficiency on the energy demand, which can be seen here as well. Due to the higher energy demand, the electricity price influence is stronger at low Faraday efficiencies.

Increasing the electricity price shifts the curves to the up-right corner towards higher required current densities and Faraday efficiencies, and the feasible region decreases considerably. The shape of the curves, however, remains the same. At higher electricity prices as displayed here, the electricity costs alone exceed the benchmark price and thus the process will not be feasible independently of the catalyst. However, the energy demands of the EHB and NRR are similar (recall Fig. 3). Therefore, high electricity costs will similarly affect the benchmark price which is assumed to be constant in this analysis. Still, this analysis shows the importance of low electricity prices for the success of ammonia production from RE.

The curve for an electricity price of  $0 \in MWh^{-1}$  represents the lowest bound for catalyst development. Such an electricity price will never be achieved for a long period. However, this curve shows the influence

of solely investment cost. Even low Faraday efficiencies can be economically feasible. This curve gives the lower bound for the required current density towards ammonia. The minimal current density is about  $60 \, \text{mA cm}^{-2}$ , which is still considerably higher than current densities achieved in literature (see Fig. 4, Figure S.2 in the SI).

Comparing the curves for  $0 \in MWh^{-1}$  and  $30 \in MWh^{-1}$  shows the stronger influence of the electricity cost compared to the investment cost, especially at lower to medium Faraday efficiencies. Increasing the electricity cost has a huge influence on the required current density. This can also be seen in Figure S.1 which shows the investment and electricity cost against the Faraday efficiency for the base case. At low Faraday efficiencies, the electricity costs are higher than the benchmark price. At the minimal Faraday efficiency, the electricity cost is still considerably higher than the investment cost. At high Faraday efficiencies, the required current density reduces, resulting in higher investment

The investment cost for electrochemical processes can only be estimated with uncertainty since there is no experience from existing NRR projects or similar projects at low TRL. Therefore, we investigate the influence on CAPEX uncertainty by altering the area- and power-dependent investment costs by +50% and -30%. Fig. 7 show this influences the cost parity curve.

The changes in the cost parity curves are comparably small compared to changes in the electricity cost or cell potential. Therefore, the influence of uncertainty in the CAPEX is considerably small and it does not influence the outcomes of this study.

The analysis of the parameter influence on the cost parity curve showed considerable changes in the position of the curve and thus the size of the feasible region for catalyst development. However, the elbow shape of the curves remains consistent. The electricity price showed a great influence on the cost parity curve, it was altered in the highest range. A more in-depth analysis of the sensitivity analysis for four distinct points from the baseline curve (green curve in Fig. 4) is given in the SI in Section S.4.

While investment costs affect both the current density and Faraday efficiency, their overall influence is relatively minor compared to the benchmark price or electricity price. The key message remains the same throughout the sensitivity analysis: for this technology to be competitive, improving the ammonia current density while achieving a sufficiently high Faraday efficiency is decisive. Faraday efficiencies close to 100% are not required.

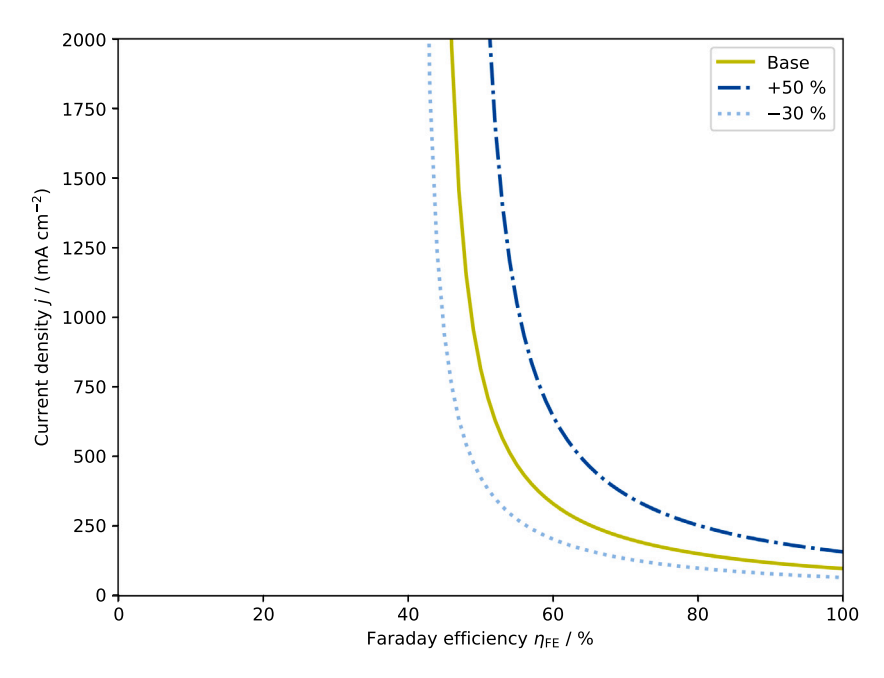


Fig. 7. Influence of uncertainty in CAPEX calculation on the cost parity curve for a benchmark price of  $c_B = 1.0 \, \mathrm{kg}_{\mathrm{NH3}}^{-1}$ , a cell potential of 2.5 V, and an electricity price of  $30 \, \mathrm{e} \, \mathrm{MWh}^{-1}$ .

#### 4.3.2. Catalyst replacement

In our analyses above, we did not account for NRR catalyst replacement costs because the durability and thus the lifetime of the catalyst is unknown. To address this limitation, we evaluate the impact of catalyst replacement on the cost parity curve by considering catalyst replacement for catalyst lifetimes of one or multiple years. The catalyst replacement is considered by including the catalyst replacement cost in the LCOA calculation (see Section S.1 in the SI).

The influence of catalyst replacement for different catalyst lifetimes on the cost parity curve is shown in Fig. 8. We assume that the catalyst must be replaced at the end of the respective lifetime. The cost of catalyst replacement is assumed to be the cathode investment cost calculated from the cost Ref. [36].

Replacing the catalyst every year moves the cost parity curve to the top right corner; higher current densities and Faraday efficiencies are required. However, the influence on the cost parity curve is lower than the uncertainty in the investment cost parameters. The effect diminishes with longer catalyst lifetimes, and the cost parity curve changes only slightly for catalyst lifetimes of three years or more.

The effect of catalyst replacement is more pronounced if the cathode and the whole stack must be replaced at the end of the catalyst lifetime (SI, Figure S.4). The required current density for a catalyst lifetime of one year is twice as high as without replacement. The effect reduces with the catalyst's lifetime, the required current density for a lifetime of two years is considerably lower.

This analysis shows the importance of catalyst durability. Catalyst replacement can have a considerable influence on the required performance if the whole stack must be replaced. The effect is stronger for shorter lifetimes. The cost parity curve changes only slightly if only the cathode must be replaced and the catalyst lifetime is three years or longer.

# 4.3.3. Selling the by-product hydrogen

The analysis showed that production at Faraday efficiencies considerably lower than 100% can be economically viable, resulting in considerable production of by-products. The main by-product is hydrogen from the HER competing with the NRR. Increasing the cell potential to increase the current density will probably affect the HER stronger than the NRR, resulting in higher hydrogen production [10].

In the previous analysis, the potential of selling the produced hydrogen is neglected, which could significantly improve the process economics since the hydrogen production costs are already accounted for in the energy demand.

How selling the hydrogen is accounted for is detailed in the SI in Section S.2. Fig. 9 shows how selling the hydrogen at a price of  $2 \in \log^{-1}$  influences the cost parity curve. It is assumed that hydrogen is the only by-product and no shunt current occurs. Thus, the amount of hydrogen produced can be calculated from the Faraday efficiency. The separation effort for producing pure hydrogen is neglected.

We ignore the separation effort and select a rather conservative hydrogen price to give a first estimate of how selling hydrogen could improve the process efficiency. Exemplary methods for hydrogen separation from gas streams containing ammonia and nitrogen are pressure swing adsorption [126] or membrane processes [127]. Operating and investment costs for these technologies will reduce the hydrogen profit but the price for green hydrogen is expected to be higher than the value assumed here. Thus, this analysis yields a first estimate of the impact of selling the by-product hydrogen.

Selling hydrogen significantly enlarges the feasible region to lower Faraday efficiencies, where a substantial amount of hydrogen is produced. The minimal Faraday efficiency is considerably lower, and the required current density at intermediate Faraday efficiencies is lower. At high Faraday efficiencies, the influence diminishes as only small quantities of hydrogen are produced relative to ammonia production, and the cost of purification at low hydrogen concentrations may outweigh the profit from sales. The minimal current density is unchanged at a Faraday efficiency of 100% (no hydrogen production).

Selling hydrogen can thus improve the performance at intermediate Faraday efficiencies and can enlarge the feasible region towards lower Faraday efficiencies. The overall picture remains the same. Compared to reported catalyst performances, considerable improvements in the current density and sufficiently high Faraday efficiencies are required. However, lower Faraday efficiencies can be sufficient if the hydrogen can be used or sold.

## 5. Discussion and implications for NRR catalyst development

This work aims to evaluate the current state of catalyst development and establish reasonable performance targets for future development,

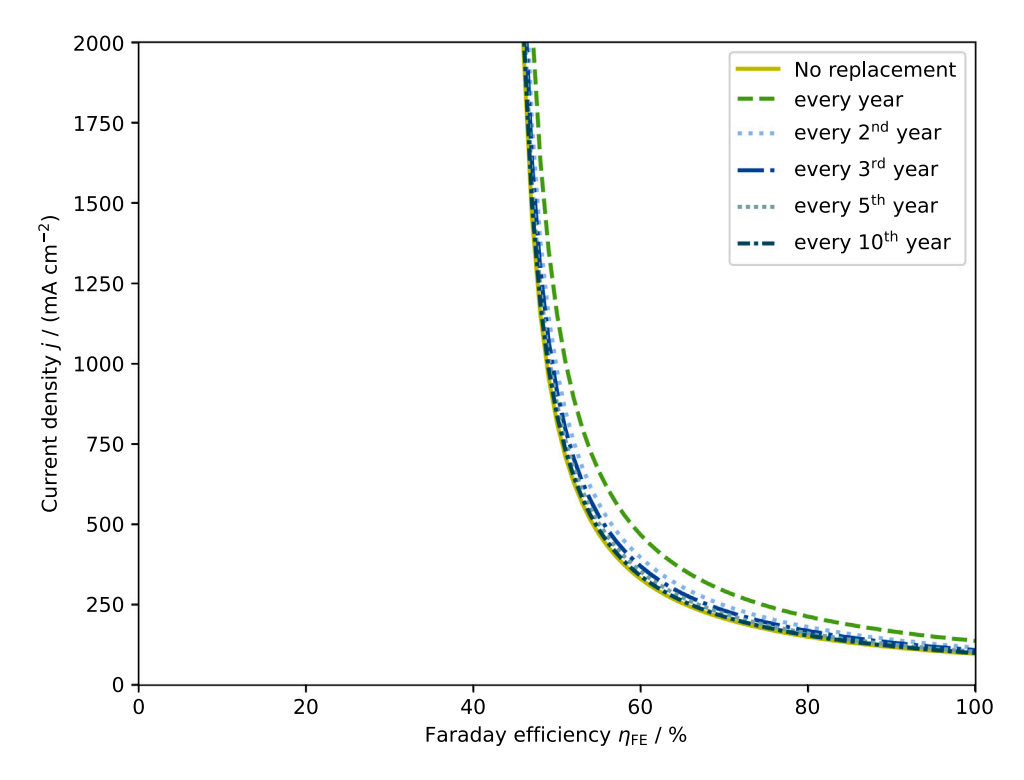


Fig. 8. Influence of catalyst replacement for different catalyst lifetimes on the cost parity curve for a benchmark price of  $c_B = 1.0 \, \mathrm{ck} \, \mathrm{g_{NH3}^{-1}}$ , a cell potential of 2.5 V, and an electricity price of  $30 \, \mathrm{cMWh^{-1}}$ .

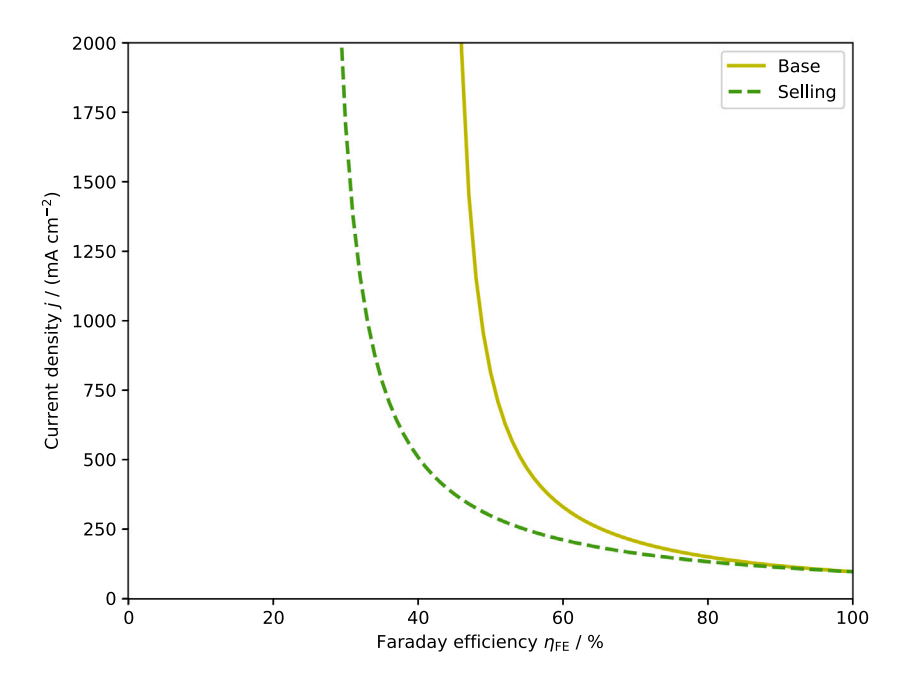


Fig. 9. Influence of selling the by-product hydrogen on the cost parity curve for a benchmark price of  $c_B = 1.0 \, \mathrm{kg}_{\mathrm{NH3}}^{-1}$ , a cell potential of 2.5 V, and an electricity price of  $30 \, \mathrm{e}\,\mathrm{MWh}^{-1}$ .

rather than assessing how these targets can be achieved. Catalyst performance data reported in the literature is well below the minimal performance levels identified in this work. While some studies achieve sufficiently high Faraday efficiencies, the current densities remain at least two orders of magnitude too low (Fig. 4, Figure S.2 in the SI). These experimental studies primarily focused on demonstrating that specific materials function as NRR catalysts and on making minor improvements to individual catalysts. Our analysis showed that catalyst development must achieve high current densities at sufficiently

high Faraday efficiencies rather than focusing on maximizing Faraday efficiencies. Reducing the cell potential is of minor importance.

Uncertainties in the parameter values of the electricity price and investment cost estimations altered the position of the cost parity curves but not the key message of the importance of the current density. Catalyst replacement has considerable influence if the whole stack must be replaced and the catalyst lifetime is low. Selling the by-product hydrogen enlarged the feasible region towards even lower Faraday efficiencies (Fig. 9). Selling hydrogen reduced the minimal Faraday

M.J. Rix and A. Mitsos Electrochimica Acta 523 (2025) 145893

efficiency and the required current density at intermediate Faraday efficiencies. However, the minimal current density did not change.

Altering the cell potential—a catalyst performance parameter—showed a low influence at high Faraday efficiencies on both required current density and Faraday efficiency. At lower Faraday efficiency, the influence is large. The energy demand is high and thus changes in the cell potential have a higher impact. Still, the current density and the Faraday efficiency have a greater impact on the catalyst performance and are therefore more important parameters. Improving them while also slightly increasing the cell potential will be beneficial for the process performance.

Recent studies state that the Faraday efficiency and thus the competing HER is the major challenge in developing the NRR (e.g., [5,9, 10,14,15]). We showed that catalyst research on increasing the current density while achieving sufficiently high Faraday efficiencies is crucial for taking the NRR process forward. We emphasize that *both* the current density and Faraday efficiency, rather than Faraday efficiency alone, are key factors for improving the process.

We investigated the individual effects of the catalyst performance parameters. However, physically, the catalyst performance parameters are interconnected. The current density can be increased by increasing the cell potential to improve the reaction kinetics. An increased cell potential is expected to have a higher influence on the HER as on the NRR and thus will reduce the Faraday efficiency [10]. Further, an increased cell potential will lead to a higher energy demand compared to the EHB process. However, we showed that the NRR process can still be competitive at higher cell potentials.

Higher current densities will lead to a fast reduction of the nitrogen availability at the catalyst. This underlines the importance of GDEs to improve nitrogen availability at the catalyst. Further experimental studies are required to improve nitrogen adsorption over water or proton adsorption at the catalyst.

Thus, the major challenge is to increase the current density while reliably achieving sufficiently high Faraday efficiencies. We demonstrated a large feasible space for the Faraday efficiency, Faraday efficiencies near 100% are not required. These outcomes are important when evaluating or publishing experimental results. Achieving high Faraday efficiencies at low current densities will only prove that a certain material can be a suitable catalyst. However, the next step must be to show that sufficiently high Faraday efficiencies can still be achieved at high current densities.

Catalyst durability is an important factor. If the catalyst must be replaced after each year or at an even higher frequency, the production costs increase and higher catalyst performances are required. The influence on the required catalyst performance is small at catalyst lifetimes of three years and longer.

Due to the one-step reaction and the lower theoretical energy demand, the NRR process has a high potential to compete with the EHB. It can be applied at smaller scales because the main equipment, the electrolyzer, benefits less from the economy of scale compared to the HB process. However, the main hurdle, improving the current density while achieving sufficiently high Faraday efficiencies must be overcome. Further, long-term studies in pilot plants will be important for proving catalyst longevity and the scalability of the process.

## 6. Conclusion and future work

We presented an approach to calculate the ammonia production cost for the NRR process depending on the performance of the NRR catalyst. As a result of this techno-economic analysis, we calculated the catalyst performance required for cost parity with benchmark prices. We calculated capital investment cost by transferring water electrolysis cost and considering technological differences. We calculated operating costs as the sum of electricity costs from the energy demand and operating and maintenance costs.

By calculating the production cost of the overall process depending on the NRR catalyst performance (current density, Faraday efficiency, and cell potential), we put recent improvements in catalyst development into perspective with requirements for an economically viable process. The resulting cost parity curves serve as performance targets for catalyst development. These targets for catalyst development are not one operation point but the feasible region above the cost parity curve. Various combinations of catalyst performance parameters result in the same production cost. We compared different catalysts and put them into perspective with benchmark prices based on current density, Faraday efficiency, and cell potential—parameters that are typically reported in catalyst studies.

The feasible region for the base case at a cell potential of  $2.5\,\mathrm{V}$  requires current densities in the range of  $100\,\mathrm{mA\,cm^{-2}}$  to  $250\,\mathrm{mA\,cm^{-2}}$  and Faraday efficiencies in the range of 60% to 100%. We show that Faraday efficiencies higher than the minimal are achieved in some studies. However, the current density is well below the minimum in all studies. Improving the current density while achieving Faraday efficiencies above the minimal will be crucial to an economically viable process. According to the literature, this will be a major challenge. Increasing the cell potential will mainly benefit the HER and thus result in small improvements in the ammonia current density but at a considerable decrease in Faraday efficiency. Therefore, finding and improving catalysts that favor the NRR over HER even at elevated potentials will be critical for the NRR process.

We investigated the influence of catalyst durability on the required performance. The required performance increased for short catalyst lifetimes but the effect diminishes at lifetimes exceeding three years. If the whole stack must be replaced, the effect is more pronounced. Still, at lifetimes exceeding three years, the effects are less than the uncertainty of the investment cost.

In addition to the catalyst level, measures at the reactor and process level can improve the performance of the NRR process. Tuned GDEs can increase the nitrogen availability at the catalyst even at higher reaction rates. Flexible operation of the process can reduce electricity costs by operating only at lower electricity prices due to the considerable influence of the electricity price on the process performance (Fig. 6). However, this will result in higher specific investment costs. The ammonia separation effort will shift the cost parity curves to the up-right corner and result in higher requirements on the catalyst performance.

An important next step is to evaluate the influence of the separation effort of ammonia and hydrogen and the infrastructure required to deliver the products to the market on the cost parity curve. There is potential for heat integration with the electrolyzer which could reduce the energy demand of the separation. Finally, using or selling hydrogen will be important at low Faraday efficiencies which can be expected at higher current densities. Therefore, investigating the hydrogen separation effort as well as potential use cases will be important. It is crucial for the NRR process that catalysts are developed and improved to achieve performances near the targets identified in this work in the near future. These catalysts should be tested in pilot plants at industrial-like conditions to validate that the NRR process can be a competing alternative to the established Haber–Bosch process.

# CRediT authorship contribution statement

**Michael J. Rix:** Writing – original draft, Visualization, Methodology, Investigation, Conceptualization. **Alexander Mitsos:** Writing – review & editing, Supervision, Project administration, Methodology, Funding acquisition, Conceptualization.

# Declaration of competing interest

The authors have no conflict of interest.

#### Acknowledgment

The authors gratefully acknowledge the financial support by the European Commission's Horizon Europe-funded project VERGE (no. 101084253).

#### Appendix A. Supplementary data

Supplementary material related to this article can be found online at https://doi.org/10.1016/j.electacta.2025.145893.

#### Data availability

No data was used for the research described in the article.

#### References

- IEA, Ammonia Technology Roadmap, IEA, 2021, https://www.iea.org/reports/ ammonia-technology-roadmap.
- [2] M. Appl, Ammonia: Principles and Industrial Practice, Wiley-VCH, Weinheim and New York, 2007, http://dx.doi.org/10.1002/9783527613885, URL https://onlinelibrary.wiley.com/doi/book/10.1002/9783527613885.
- [3] C. Smith, A.K. Hill, L. Torrente-Murciano, Current and future role of Haber-Bosch ammonia in a carbon-free energy landscape, Energy Environ. Sci. 13 (2) (2020) 331–344, http://dx.doi.org/10.1039/C9EE02873K.
- [4] D.R. MacFarlane, P.V. Cherepanov, J. Choi, B.H. Suryanto, R.Y. Hodgetts, J.M. Bakker, F.M. Ferrero Vallana, A.N. Simonov, A roadmap to the ammonia economy, Joule 4 (6) (2020) 1186–1205, http://dx.doi.org/10.1016/j.joule. 2020.04.004.
- [5] F. Rezaie, S. Læsaa, N.E. Sahin, J. Catalano, E. Dražević, Low-temperature electrochemical ammonia synthesis: Measurement reliability and comparison to Haber-Bosch in terms of energy efficiency, Energy Technol. 11 (10) (2023) 2300410, http://dx.doi.org/10.1002/ente.202300410.
- [6] S. Li, Y. Zhou, X. Fu, J.B. Pedersen, M. Saccoccio, S.Z. Andersen, K. Enemark-Rasmussen, P.J. Kempen, C.D. Damsgaard, A. Xu, R. Sažinas, J.B.V. Mygind, N.H. Deissler, J. Kibsgaard, P.C.K. Vesborg, J.K. Nørskov, I. Chorkendorff, Longterm continuous ammonia electrosynthesis, Nature 629 (8010) (2024) 92–97, http://dx.doi.org/10.1038/s41586-024-07276-5.
- [7] G. Qing, R. Ghazfar, S.T. Jackowski, F. Habibzadeh, M.M. Ashtiani, C.-P. Chen, M.R. Smith, T.W. Hamann, Recent advances and challenges of electrocatalytic N2 reduction to ammonia, Chem. Rev. 120 (12) (2020) 5437–5516, http://dx.doi.org/10.1021/acs.chemrev.9b00659.
- [8] T. Wu, W. Fan, Y. Zhang, F. Zhang, Electrochemical synthesis of ammonia: Progress and challenges, Mater. Today Phys. 16 (2021) 100310, http://dx.doi. org/10.1016/j.mtphys.2020.100310.
- [9] G.F. Chen, S. Ren, L. Zhang, H. Cheng, Y. Luo, K. Zhu, L.X. Ding, H. Wang, Advances in electrocatalytic N 2 reduction—Strategies to tackle the selectivity challenge, Small Methods 3 (6) (2019) 1800337, http://dx.doi.org/10.1002/ smtd.201800337, URL https://onlinelibrary.wiley.com/doi/full/10.1002/smtd. 201800337.
- [10] A.R. Singh, B.A. Rohr, J.A. Schwalbe, M. Cargnello, K. Chan, T.F. Jaramillo, I. Chorkendorff, J.K. Nørskov, Electrochemical ammonia synthesis—The selectivity challenge, ACS Catal. 7 (1) (2017) 706–709, http://dx.doi.org/10.1021/ acscatal.6b03035.
- [11] A.N. Singh, R. Anand, M. Zafari, M. Ha, K.S. Kim, Progress in single/multi atoms and 2D-nanomaterials for electro/photocatalytic nitrogen reduction: Experimental, computational and machine leaning developments, Adv. Energy Mater. (2024) 2304106, http://dx.doi.org/10.1002/aenm.202304106, URL https://onlinelibrary.wiley.com/doi/full/10.1002/aenm.202304106.
- [12] H. Xu, K. Ithisuphalap, Y. Li, S. Mukherjee, J. Lattimer, G. Soloveichik, G. Wu, Electrochemical ammonia synthesis through N2 and H2O under ambient conditions: Theory, practices, and challenges for catalysts and electrolytes, Nano Energy 69 (2020) 104469, http://dx.doi.org/10.1016/j.nanoen.2020.104469, URL https://www.sciencedirect.com/science/article/pii/S2211285520300252.
- [13] B. Chang, H. Zhang, S. Sun, G. Zhang, Strategies to achieve effective nitrogen activation, Carbon Energy (2024) e491, http://dx.doi.org/10.1002/cey2.491.
- [14] L. Hu, Z. Xing, X. Feng, Understanding the electrocatalytic interface for ambient ammonia synthesis, ACS Energy Lett. 5 (2) (2020) 430–436, http://dx.doi.org/ 10.1021/acsenergylett.9b02679.
- [15] Y. Ren, C. Yu, X. Tan, H. Huang, Q. Wei, J. Qiu, Strategies to suppress hydrogen evolution for highly selective electrocatalytic nitrogen reduction: challenges and perspectives, Energy Environ. Sci. 14 (3) (2021) 1176–1193, http://dx.doi.org/10.1039/D0EE03596C.

- [16] G. Hochman, A.S. Goldman, F.A. Felder, J.M. Mayer, A.J.M. Miller, P.L. Holland, L.A. Goldman, P. Manocha, Z. Song, S. Aleti, Potential economic feasibility of direct electrochemical nitrogen reduction as a route to ammonia, ACS Sustain. Chem. Eng. 8 (24) (2020) 8938–8948, http://dx.doi.org/10.1021/acssuschem.eng. 0c01206
- [17] C.A. Fernandez, M.C. Hatzell, Editors' choice—Economic considerations for low-temperature electrochemical ammonia production: Achieving haber-bosch parity, J. Electrochem. Soc. 167 (14) (2020) 143504, http://dx.doi.org/ 10.1149/1945-7111/abc35b, URL https://iopscience.iop.org/article/10.1149/ 1945-7111/abc35b.
- [18] M. Wang, M.A. Khan, I. Mohsin, J. Wicks, A.H. Ip, K.Z. Sumon, C.-T. Dinh, E.H. Sargent, I.D. Gates, M.G. Kibria, Can sustainable ammonia synthesis pathways compete with fossil-fuel based Haber–Bosch processes? Energy Environ. Sci. 14 (5) (2021) 2535–2548, http://dx.doi.org/10.1039/D0EE03808C.
- [19] M. Kim, D. Lee, M. Qi, J. Kim, Techno-economic analysis of anion exchange membrane electrolysis process for green hydrogen production under uncertainty, Energy Convers. Manage. 302 (2024) 118134, http://dx.doi.org/10. 1016/j.enconman.2024.118134, URL https://www.sciencedirect.com/science/ article/pii/S019689042400075X.
- [20] J. Na, B. Seo, J. Kim, C.W. Lee, H. Lee, Y.J. Hwang, B.K. Min, D.K. Lee, H.-S. Oh, U. Lee, General technoeconomic analysis for electrochemical coproduction coupling carbon dioxide reduction with organic oxidation, Nat. Commun. 10 (1) (2019) 5193, http://dx.doi.org/10.1038/s41467-019-12744-y, URL https://www.nature.com/articles/s41467-019-12744-y#Sec10.
- [21] M. Moreno-Gonzalez, A. Berger, T. Borsboom-Hanson, W. Mérida, Carbonneutral fuels and chemicals: Economic analysis of renewable syngas pathways via CO2 electrolysis, Energy Convers. Manage. 244 (2021) 114452, http:// dx.doi.org/10.1016/j.enconman.2021.114452, URL https://www.sciencedirect. com/science/article/pii/S0196890421006282.
- [22] X. Li, P. Anderson, H.-R.M. Jhong, M. Paster, J.F. Stubbins, P.J.A. Kenis, Greenhouse gas emissions, energy efficiency, and cost of synthetic fuel production using electrochemical CO 2 conversion and the Fischer–Tropsch process, Energy Fuels 30 (7) (2016) 5980–5989, http://dx.doi.org/10.1021/acs.energyfuels. 6b00665.
- [23] J.M. Spurgeon, B. Kumar, A comparative technoeconomic analysis of pathways for commercial electrochemical CO 2 reduction to liquid products, Energy Environ. Sci. 11 (6) (2018) 1536–1551, http://dx.doi.org/10.1039/C8EE00097B, URL https://pubs.rsc.org/en/content/articlehtml/2018/ee/c8ee00097b.
- [24] M. Jouny, W. Luc, F. Jiao, General techno-economic analysis of CO 2 electrolysis systems, Ind. Eng. Chem. Res. 57 (6) (2018) 2165–2177, http://dx.doi.org/10. 1021/acs.jecr.7b03514.
- [25] A. Mitsos, B. Chachuat, P.I. Barton, Methodology for the design of man-portable power generation devices, Ind. Eng. Chem. Res. 46 (22) (2007) 7164–7176, http://dx.doi.org/10.1021/ie070586z.
- [26] M. Jouny, W. Luc, F. Jiao, General techno-economic analysis of CO2 electrolysis systems, Ind. Eng. Chem. Res. 57 (6) (2018) 2165–2177, http://dx.doi.org/10. 1021/acs.jecr.7b03514.
- [27] A. Cruellas, J. Bakker, M. van Sint Annaland, J. Medrano, F. Gallucci, Technoeconomic analysis of oxidative coupling of methane: Current state of the art and future perspectives, Energy Convers. Manage. 198 (2019) 111789, http:// dx.doi.org/10.1016/j.enconman.2019.111789, URL https://www.sciencedirect. com/science/article/pii/S019689041930771X.
- [28] S. Mucci, M.-D. Stumm, M.J. Rix, A. Mitsos, Model-based evaluation of ammonia energy storage concepts at high technological readiness level, Appl. Energy 377 (2025) 124495, http://dx.doi.org/10.1016/j.apenergy.2024.124495, URL https://www.sciencedirect.com/science/article/pii/S0306261924018786.
- [29] G. Wang, A. Mitsos, W. Marquardt, Conceptual design of ammonia-based energy storage system: System design and time-invariant performance, AIChE J. 63 (5) (2017) 1620–1637, http://dx.doi.org/10.1002/aic.15660, URL https://aiche.onlinelibrary.wiley.com/doi/abs/10.1002/aic.15660.
- [30] X. He, Y. Liao, J. Tan, G. Li, F. Yin, Defective UiO-66 toward boosted electrochemical nitrogen reduction to ammonia, Electrochim. Acta 409 (2022) 139988, http://dx.doi.org/10.1016/j.electacta.2022.139988.
- [31] X. Li, Y. Yang, B. Yue, J. Lin, Q. Hu, P. Li, Y. Liu, L. Duan, Q. Zhuang, Y. Wang, J. Liu, Microstructure regulation of carbon nitrides for electrochemical nitrogen fixation, Electrochim. Acta 466 (2023) 143056, http://dx.doi.org/10.1016/j.electacta.2023.143056.
- [32] J. Wei, Y. Jing, Z. Zhao, Z. Fan, Z. Liang, J. Huang, H. Wu, Z. Xie, D. Liu, D. Qu, H. Tang, J. Li, Catalyst-Support interactions enhanced electrochemical nitrogen reduction on Au/ZrO2, Electrochim. Acta 381 (2021) 138222, http://dx.doi.org/10.1016/j.electacta.2021.138222, URL https://www.sciencedirect.com/science/article/pii/S0013468621005120.
- [33] G. Sakas, A. Ibáñez Rioja, S. Pöyhönen, A. Kosonen, V. Ruuskanen, P. Kauranen, J. Ahola, Influence of shunt currents in industrial-scale alkaline water electrolyzer plants, Renew. Energy 225 (2024) 120266, http://dx.doi.org/10.1016/j.renene.2024.120266, URL https://www.sciencedirect.com/science/article/pii/S0960148124003318.
- [34] J. Hemauer, S. Rehfeldt, H. Klein, A. Peschel, Performance and cost modelling taking into account the uncertainties and sensitivities of current and nextgeneration PEM water electrolysis technology, Int. J. Hydrog. Energy 48 (2023)

- $\label{eq:25619-25634} 25619-25634, \ http://dx.doi.org/10.1016/j.ijhydene.2023.03.050, \ URL \ https://www.sciencedirect.com/science/article/pii/S0360319923010650.$
- [35] IRENA, Green Hydrogen Cost Reduction: Scaling up Electrolysers to Meet the 1.5 °C Climate Goal, International Renewable Energy Agency, Abu Dhabi, 2020.
- [36] M. Holst, S. Aschbrenner, T. Smolinka, C. Voglstätter, G. Grimm, Cost Forecast for Low Temperature Electrolysis - Technology Driven Bottom-Up Prognosis for PEM and Alkaline Water Electrolysis Systems, Fraunhofer ISE, 2021, http:// dx.doi.org/10.24406/publica-1318, URL https://publica.fraunhofer.de/handle/ publica/441376.
- [37] S. Skribbe, M. Liu, S. Patel, M.J. Rix, F. Bensebaa, L. Mak, X.-Y. Wu, The levelized cost of carbon abatement (LCCA) in substituting conventional ammonia production with power-to-ammonia for fertilizer, hydrogen and export, Appl. Energy 373 (2024) 123859, http://dx.doi.org/10.1016/ j.apenergy.2024.123859, URL https://www.sciencedirect.com/science/article/ pii/S030626192401242X.
- [38] F. Cameli, A. Kourou, V. Rosa, E. Delikonstantis, V. Galvita, K.M. Van Geem, G.D. Stefanidis, Conceptual process design and technoeconomic analysis of an e-ammonia plant: Green H2 and cryogenic air separation coupled with Haber-Bosch process, Int. J. Hydrog. Energy 49 (2024) 1416–1425, http://dx.doi.org/10.1016/j.ijhydene.2023.10.020, URL https://www.sciencedirect.com/science/article/pii/S036031992305084X.
- [39] Y. Abghoui, A.L. Garden, V.F. Hlynsson, S. Björgvinsdóttir, H. Ólafsdóttir, E. Skúlason, Enabling electrochemical reduction of nitrogen to ammonia at ambient conditions through rational catalyst design, Phys. Chem. Chem. Phys. 17 (7) (2015) 4909–4918, http://dx.doi.org/10.1039/c4cp04838e.
- [40] A. Biswas, S. Kapse, B. Ghosh, R. Thapa, R.S. Dey, Lewis acid-dominated aqueous electrolyte acting as co-catalyst and overcoming N2 activation issues on catalyst surface, Proc. Natl. Acad. Sci. USA 119 (33) (2022) e2204638119, http://dx.doi.org/10.1073/pnas.2204638119.
- [41] W. Cai, Y. Han, H. Li, W. Qi, J. Xu, X. Wu, H. Zhao, X. Zhang, J. Lai, L. Wang, Significantly enhanced electrocatalytic N2 reduction to NH3 by surface selenization with multiple functions, J. Mater. Chem. A 8 (39) (2020) 20331–20336, http://dx.doi.org/10.1039/D0TA06991D.
- [42] W. Cai, Y. Han, Y. Pan, X. Zhang, J. Xu, Y. Zhang, Y. Sun, S. Li, J. Lai, L. Wang, The twinned pd nanocatalyst exhibits sustainable NRR electrocatalytic performance by promoting the desorption of NH3, J. Mater. Chem. A 9 (23) (2021) 13483–13489, http://dx.doi.org/10.1039/D1TA02720D.
- [43] Y. Chen, R. Guo, X. Peng, X. Wang, X. Liu, J. Ren, J. He, L. Zhuo, J. Sun, Y. Liu, Y. Wu, J. Luo, Highly productive electrosynthesis of ammonia by admolecule-targeting single ag sites, ACS Nano 14 (6) (2020) 6938–6946, http://dx.doi.org/10.1021/acsnano.0c01340.
- [44] J. Chen, C. Zhang, M. Huang, J. Zhang, J. Zhang, H. Liu, G. Wang, R. Wang, The activation of porous atomic layered MoS2 basal-plane to induce adjacent Mo atom pairs promoting high efficiency electrochemical N2 fixation, Appl. Catal. B: Environ. 285 (2021) 119810, http://dx.doi.org/10.1016/j.apcatb. 2020.119810.
- [45] K. Chu, Y.-p. Liu, Y.-h. Cheng, Q.-q. Li, Synergistic boron-dopants and boron-induced oxygen vacancies in MnO2 nanosheets to promote electrocatalytic nitrogen reduction, J. Mater. Chem. A 8 (10) (2020) 5200–5208, http://dx.doi.org/10.1039/D0TA00220H.
- [46] K. Chu, Q.-q. Li, Y.-h. Cheng, Y.-p. Liu, Efficient electrocatalytic nitrogen fixation on FeMoO4 nanorods, ACS Appl. Mater. Interfaces 12 (10) (2020) 11789–11796, http://dx.doi.org/10.1021/acsami.0c00860.
- [47] K. Chu, J. Wang, Y.-p. Liu, Q.-q. Li, Y.-l. Guo, Mo-doped SnS2 with enriched S-vacancies for highly efficient electrocatalytic N2 reduction: the critical role of the Mo-Sn-Sn trimer, J. Mater. Chem. A 8 (15) (2020) 7117–7124, http: //dx.doi.org/10.1039/D0TA01688H.
- [48] K. Chu, Y.-p. Liu, Y.-b. Li, Y.-l. Guo, Y. Tian, H. Zhang, Multi-functional Mo-doping in MnO2 nanoflowers toward efficient and robust electrocatalytic nitrogen fixation, Appl. Catal. B: Environ. 264 (2020) 118525, http://dx.doi. org/10.1016/j.apcatb.2019.118525.
- [49] S. Chung, H. Ju, M. Choi, D. Yoon, J. Lee, Local proton source enhanced nitrogen reduction on a combined cobalt-molybdenum catalyst for electrochemical ammonia synthesis, Angew. Chem. (Int. Ed. English) 61 (47) (2022) e202212676, http://dx.doi.org/10.1002/anie.202212676.
- [50] C. Du, C. Qiu, Z. Fang, P. Li, Y. Gao, J. Wang, W. Chen, Interface hydrophobic tunnel engineering: A general strategy to boost electrochemical conversion of N2 to NH3, Nano Energy 92 (2022) 106784, http://dx.doi.org/10.1016/j. nanoen.2021.106784.
- [51] W. Fang, J. Zhao, T. Wu, Y. Huang, L. Yang, C. Liu, Q. Zhang, K. Huang, Q. Yan, Hydrophilic engineering of VOx-based nanosheets for ambient electrochemical ammonia synthesis at neutral pH, J. Mater. Chem. A 8 (12) (2020) 5913–5918, http://dx.doi.org/10.1039/D0TA00676A.
- [52] Y. Fang, Y. Xue, L. Hui, H. Yu, C. Zhang, B. Huang, Y. Li, Graphdiyne-induced iron vacancy for efficient nitrogen conversion, Adv. Sci. 9 (2) (2022) e2102721, http://dx.doi.org/10.1002/advs.202102721.
- [53] Y. Fu, T. Li, G. Zhou, J. Guo, Y. Ao, Y. Hu, J. Shen, L. Liu, X. Wu, Dual-metal-driven selective pathway of nitrogen reduction in orderly atomic-hybridized Re2MnS6 ultrathin nanosheets, Nano Lett. 20 (7) (2020) 4960–4967, http://dx.doi.org/10.1021/acs.nanolett.0c01037.

- [54] U.K. Ghorai, S. Paul, B. Ghorai, A. Adalder, S. Kapse, R. Thapa, A. Nagendra, A. Gain, Scalable production of cobalt phthalocyanine nanotubes: Efficient and robust hollow electrocatalyst for ammonia synthesis at room temperature, ACS Nano 15 (3) (2021) 5230–5239, http://dx.doi.org/10.1021/acsnano.0c10596.
- [55] Y. Guo, T. Wang, Q. Yang, X. Li, H. Li, Y. Wang, T. Jiao, Z. Huang, B. Dong, W. Zhang, J. Fan, C. Zhi, Highly efficient electrochemical reduction of nitrogen to ammonia on surface termination modified Ti3C2Tx MXene nanosheets, ACS Nano 14 (7) (2020) 9089–9097, http://dx.doi.org/10.1021/acsnano.0c04284.
- [56] Y. Guo, J. Liu, Q. Yang, P. Khemthong, Z. Huang, Y. Zhao, Z. Chen, B. Dong, X.-Z. Fu, J.-L. Luo, C. Zhi, Regulating nitrogenous adsorption and desorption on Pd clusters by the acetylene linkages of hydrogen substituted graphdiyne for efficient electrocatalytic ammonia synthesis, Nano Energy 86 (2021) 106099, http://dx.doi.org/10.1016/j.nanoen.2021.106099.
- [57] Y. Guo, Y. Cheng, Q. Li, K. Chu, FeTe2 as an earth-abundant metal telluride catalyst for electrocatalytic nitrogen fixation, J. Energy Chem. 56 (2021) 259–263, http://dx.doi.org/10.1016/j.jechem.2020.07.055.
- [58] D. Gupta, A. Kafle, S. Kaur, P.P. Mohanty, T. Das, S. Chakraborty, R. Ahuja, T.C. Nagaiah, High yield selective electrochemical conversion of N2 to NH3via morphology controlled silver phosphate under ambient conditions, J. Mater. Chem. A 10 (38) (2022) 20616–20625, http://dx.doi.org/10.1039/D2TA04155C.
- [59] M. Han, M. Guo, Y. Yun, Y. Xu, H. Sheng, Y. Chen, Y. Du, K. Ni, Y. Zhu, M. Zhu, Effect of heteroatom and charge reconstruction in atomically precise metal nanoclusters on electrochemical synthesis of ammonia, Adv. Funct. Mater. 32 (29) (2022) 2202820, http://dx.doi.org/10.1002/adfm.202202820.
- [60] Y.J. Jang, K.-S. Choi, Enabling electrochemical N2 reduction to NH3 in the low overpotential region using non-noble metal bi electrodes via surface composition modification, J. Mater. Chem. A 8 (27) (2020) 13842–13851, http://dx.doi.org/10.1039/D0TA02550J.
- [61] Z. Jin, C. Liu, Z. Liu, J. Han, Y. Fang, Y. Han, Y. Niu, Y. Wu, C. Sun, Y. Xu, Rational design of hydroxyl-rich Ti3C2Tx MXene quantum dots for high-performance electrochemical N2 reduction, Adv. Energy Mater. 10 (22) (2020) 2000797, http://dx.doi.org/10.1002/aenm.202000797.
- [62] A. Kafle, D. Gupta, A. Bordoloi, T.C. Nagaiah, Self-standing Fe3O4 decorated paper electrode as a binder-free trifunctional electrode for electrochemical ammonia synthesis and Zn-O2 batteries, Nanoscale 14 (44) (2022) 16590–16601, http://dx.doi.org/10.1039/d2nr03297j.
- [63] K. Chu, Y. hua Chen, Q. qing Li, Y. ping Liu, Y. Tian, Fe-doping induced morphology change, oxygen vacancy and Ce3+-Ce3+ pairs in CeO2 for promoted electrocatalytic nitrogen fixation, J. Mater. Chem. A 8 (12) (2020) 5865–5873, http://dx.doi.org/10.1039/C9TA14260F.
- [64] J.H. Kim, H. Ju, B.-S. An, Y. An, K. Cho, S.H. Kim, Y.-S. Bae, H.C. Yoon, Comparison between Fe2O3/C and Fe3C/Fe2O3/Fe/C Electrocatalysts for N2 Reduction in an Alkaline Electrolyte, ACS Appl. Mater. Interfaces 13 (51) (2021) 61316–61323, http://dx.doi.org/10.1021/acsami.1c20807.
- [65] H.S. Kim, H. Jin, S.-H. Kim, J. Choi, D.W. Lee, H.C. Ham, S.J. Yoo, H.S. Park, Sacrificial dopant to enhance the activity and durability of electrochemical N2 reduction catalysis, ACS Catal. 12 (9) (2022) 5684–5697, http://dx.doi.org/10. 1021/acscatal.2c00089.
- [66] Y. Kong, Y. Li, X. Sang, B. Yang, Z. Li, S. Zheng, Q. Zhang, S. Yao, X. Yang, L. Lei, S. Zhou, G. Wu, Y. Hou, Atomically dispersed Zinc(I) active sites to accelerate nitrogen reduction kinetics for ammonia electrosynthesis, Adv. Mater. 34 (2) (2022) e2103548, http://dx.doi.org/10.1002/adma.202103548.
- [67] F. Lai, J. Feng, X. Ye, W. Zong, G. He, C. Yang, W. Wang, Y.-E. Miao, B. Pan, W. Yan, T. Liu, I.P. Parkin, Oxygen vacancy engineering in spinel-structured nanosheet wrapped hollow polyhedra for electrochemical nitrogen fixation under ambient conditions, J. Mater. Chem. A 8 (4) (2020) 1652–1659, http://dx.doi.org/10.1039/C9TA11408D.
- [68] F. Lai, N. Chen, X. Ye, G. He, W. Zong, K.B. Holt, B. Pan, I.P. Parkin, T. Liu, R. Chen, Refining energy levels in ReS2 nanosheets by low-Valent transition-metal doping for dual-boosted electrochemical ammonia/hydrogen production, Adv. Funct. Mater. 30 (11) (2020) 1907376, http://dx.doi.org/10.1002/adfm.
- [69] Q. Li, X. Chen, Y. Yang, Biomass-derived nitrogen-doped porous carbon for highly efficient ambient electro-synthesis of NH3, Catalysts 10 (3) (2020) 353, http://dx.doi.org/10.3390/catal10030353.
- [70] Q. Li, J. Wang, Y. Cheng, K. Chu, Zn nanosheets: An earth-abundant metallic catalyst for efficient electrochemical ammonia synthesis, J. Energy Chem. 54 (2021) 318–322, http://dx.doi.org/10.1016/j.jechem.2020.06.011.
- [71] T. Li, J. Xia, Q. Chen, K. Xu, Y. Gu, Q. Liu, Y. Luo, H. Guo, E. Traversa, Monodisperse Cu cluster-loaded defective ZrO2 nanofibers for ambient N2 fixation to NH3, ACS Appl. Mater. Interfaces 13 (34) (2021) 40724–40730, http://dx.doi.org/10.1021/acsami.1c12279.
- [72] C. Li, M. Wang, L. Ren, H. Sun, Promoting the formation of oxygen vacancies in ceria multishelled hollow microspheres by doping iron for enhanced ambient ammonia electrosynthesis, Inorg. Chem. Front. 9 (7) (2022) 1467–1473, http://dx.doi.org/10.1039/D1QI01539G.
- [73] W. Liao, H.-X. Liu, L. Qi, S. Liang, Y. Luo, F. Liu, X. Wang, C.-R. Chang, J. Zhang, L. Jiang, Lithium/bismuth co-functionalized phosphotungstic acid catalyst for promoting dinitrogen electroreduction with high Faradaic efficiency, Cell Rep. Phys. Sci. 2 (9) (2021) 100557, http://dx.doi.org/10.1016/j.xcrp. 2021.100557.

- [74] G. Lin, Q. Ju, X. Guo, W. Zhao, S. Adimi, J. Ye, Q. Bi, J. Wang, M. Yang, F. Huang, Intrinsic electron localization of metastable MoS2 boosts electrocatalytic nitrogen reduction to ammonia, Adv. Mater. 33 (32) (2021) e2007509, http://dx.doi.org/10.1002/adma.202007509.
- [75] Y. Liu, Y. Luo, Q. Li, J. Wang, K. Chu, Bimetallic MnMoO4 with dual-active-centers for highly efficient electrochemical N2 fixation, Chem. Commun. 56 (70) (2020) 10227–10230, http://dx.doi.org/10.1039/d0cc04340k.
- [76] B. Liu, Y. Zheng, H.-Q. Peng, B. Ji, Y. Yang, Y. Tang, C.-S. Lee, W. Zhang, Nanostructured and boron-doped diamond as an electrocatalyst for nitrogen fixation, ACS Energy Lett. 5 (8) (2020) 2590–2596, http://dx.doi.org/10.1021/ acsenergylett.0c01317.
- [77] Q. Liu, X. Zhang, J. Wang, Y. Zhang, S. Bian, Z. Cheng, N. Kang, H. Huang, S. Gu, Y. Wang, D. Liu, P.K. Chu, X.-F. Yu, Crystalline red phosphorus nanorib-bons: Large-scale synthesis and electrochemical nitrogen fixation, Angew. Chem. (Int. Ed. English) 59 (34) (2020) 14383–14387, http://dx.doi.org/10.1002/anie.202006679.
- [78] S. Liu, T. Qian, M. Wang, H. Ji, X. Shen, C. Wang, C. Yan, Proton-filtering covalent organic frameworks with superior nitrogen penetration flux promote ambient ammonia synthesis, Nat. Catal. 4 (4) (2021) 322–331, http://dx.doi. org/10.1038/s41929-021-00599-w.
- [79] Y.-X. Luo, W.-B. Qiu, R.-P. Liang, X.-H. Xia, J.-D. Qiu, Mo-doped FeP nanospheres for artificial nitrogen fixation, ACS Appl. Mater. Interfaces 12 (15) (2020) 17452–17458, http://dx.doi.org/10.1021/acsami.0c00011.
- [80] S. Luo, X. Li, M. Wang, X. Zhang, W. Gao, S. Su, G. Liu, M. Luo, Long-term electrocatalytic N<sub>2</sub> fixation by MOF-derived Y-stabilized ZrO<sub>2</sub>: insight into the deactivation mechanism, J. Mater. Chem. A 8 (11) (2020) 5647–5654, http://dx.doi.org/10.1039/D0TA01154A.
- [81] S. Luo, X. Li, W. Gao, H. Zhang, M. Luo, An MOF-derived C@NiO@Ni electrocatalyst for N<sub>2</sub>conversion to NH<sub>3</sub>in alkaline electrolytes, Sustain. Energy Fuels 4 (1) (2020) 164–170, http://dx.doi.org/10.1039/C9SE00691E.
- [82] X.-W. Lv, X.-L. Liu, Y.-J. Suo, Y.-P. Liu, Z.-Y. Yuan, Identifying the dominant role of pyridinic-N-Mo bonding in synergistic electrocatalysis for ambient nitrogen reduction, ACS Nano 15 (7) (2021) 12109–12118, http://dx.doi.org/10.1021/ acsnano.1c03465.
- [83] X.-W. Lv, X.-L. Liu, L.-J. Gao, Y.-P. Liu, Z.-Y. Yuan, Iron-doped titanium dioxide hollow nanospheres for efficient nitrogen fixation and Zn-N2 aqueous batteries, J. Mater. Chem. A 9 (7) (2021) 4026–4035, http://dx.doi.org/10. 1039/D0TA11244E.
- [84] X. Ma, Q. Zhang, L. Gao, Y. Zhang, C. Hu, Atomic-layer-deposited oxygen-deficient TiO2 on carbon cloth: An efficient electrocatalyst for nitrogen fixation, ChemCatChem 14 (19) (2022) e202200756, http://dx.doi.org/10.1002/cctc. 202200756
- [85] X. Ma, S. Yan, W. Yi, J. He, L. Yi, Prussian blue-derived Fe@NC as an efficient electrocatalyst for ammonia synthesis under ambient conditions, ACS Sustain. Chem. Eng. 10 (37) (2022) 12148–12155, http://dx.doi.org/10.1021/ acssuschemeng.2c02596.
- [86] M. Nazemi, P. Ou, A. Alabbady, L. Soule, A. Liu, J. Song, T.A. Sulchek, M. Liu, M.A. El-Sayed, Electrosynthesis of ammonia using porous bimetallic Pd-Ag nanocatalysts in liquid- and gas-phase systems, ACS Catal. 10 (17) (2020) 10197–10206, http://dx.doi.org/10.1021/acscatal.0c02680.
- [87] M. Nazemi, L. Soule, M. Liu, M.A. El-Sayed, Ambient ammonia electrosynthesis from nitrogen and water by incorporating palladium in bimetallic gold–silver nanocages, J. Electrochem. Soc. 167 (5) (2020) 054511, http://dx.doi.org/10. 1149/1945-7111/ab6ee9.
- [88] S.B. Patil, H.-L. Chou, Y.-M. Chen, S.-H. Hsieh, C.-H. Chen, C.-C. Chang, S.-R. Li, Y.-C. Lee, Y.-S. Lin, H. Li, Y.J. Chang, Y.-H. Lai, D.-Y. Wang, Enhanced N2 affinity of 1T-MoS2 with a unique pseudo-six-membered ring consisting of N-Li-S-Mo-S-Mo for high ambient ammonia electrosynthesis performance, J. Mater. Chem. A 9 (2) (2021) 1230–1239, http://dx.doi.org/10.1039/D0TA10696H.
- [89] W. Qiu, Y.-X. Luo, R.-P. Liang, J.-D. Qiu, Amorphous/crystalline heterophase TiO2-coated  $\alpha$ -Fe2O3 core–shell nanospindles: A high-performance artificial nitrogen fixation electrocatalyst, Chem. A Eur. J. 26 (45) (2020) 10226–10229, http://dx.doi.org/10.1002/chem.202000695, URL https://chemistry-europe.onlinelibrary.wiley.com/doi/abs/10.1002/chem.202000695.
- [90] P. Shen, X. Li, Y. Luo, Y. Guo, X. Zhao, K. Chu, High-efficiency N2 electroreduction enabled by Se-vacancy-rich WSe2-x in water-in-salt electrolytes, ACS Nano 16 (5) (2022) 7915–7925, http://dx.doi.org/10.1021/acsnano.2c00596.
- [91] P. Shen, X. Li, Y. Luo, N. Zhang, X. Zhao, K. Chu, Ultra-efficient N2 electroreduction achieved over a rhodium single-atom catalyst (Rh1/MnO2) in water-in-salt electrolyte, Appl. Catal. B: Environ. 316 (2022) 121651, http://dx.doi.org/10.1016/j.apcatb.2022.121651.
- [92] L. Shi, S. Bi, Y. Qi, R. He, K. Ren, L. Zheng, J. Wang, G. Ning, J. Ye, Anchoring Mo single-atom sites on B/N codoped porous carbon nanotubes for electrochemical reduction of N2 to NH3, ACS Catal. 12 (13) (2022) 7655–7663, http://dx.doi.org/10.1021/acscatal.2c01293.
- [93] Y. Tian, X. Shao, M. Zhu, W. Liu, Z. Wei, K. Chu, A spinel ferrite catalyst for efficient electroreduction of dinitrogen to ammonia, Dalton Trans. 49 (36) (2020) 12559–12564, http://dx.doi.org/10.1039/d0dt02560g.

- [94] Y. Tian, B. Chang, G. Wang, L. Li, L. Gong, B. Wang, R. Yuan, W. Zhou, Magnetron sputtering tuned "π back-donation" sites over metal oxides for enhanced electrocatalytic nitrogen reduction, J. Mater. Chem. A 10 (6) (2022) 2800–2806, http://dx.doi.org/10.1039/d1ta10273g.
- [95] Y. Wan, H. Zhou, M. Zheng, Z.-H. Huang, F. Kang, J. Li, R. Lv, Oxidation state modulation of bismuth for efficient electrocatalytic nitrogen reduction to ammonia, Adv. Funct. Mater. 31 (30) (2021) 2100300, http://dx.doi.org/10. 1002/adfm.202100300.
- [96] H.-B. Wang, J.-Q. Wang, R. Zhang, C.-Q. Cheng, K.-W. Qiu, Y.-j. Yang, J. Mao, H. Liu, M. Du, C.-K. Dong, X.-W. Du, Bionic design of a Mo(IV)-doped FeS2 catalyst for electroreduction of dinitrogen to ammonia, ACS Catal. 10 (9) (2020) 4914–4921, http://dx.doi.org/10.1021/acscatal.0c00271.
- [97] Y. Wang, A. Chen, S. Lai, X. Peng, S. Zhao, G. Hu, Y. Qiu, J. Ren, X. Liu, J. Luo, Self-supported NbSe2 nanosheet arrays for highly efficient ammonia electrosynthesis under ambient conditions, J. Catalysis 381 (2020) 78–83, http://dx.doi.org/10.1016/j.jcat.2019.10.029.
- [98] M. Wang, S. Liu, H. Ji, T. Yang, T. Qian, C. Yan, Salting-out effect promoting highly efficient ambient ammonia synthesis, Nat. Commun. 12 (1) (2021) 3198, http://dx.doi.org/10.1038/s41467-021-23360-0.
- [99] Phosphorus modulation of a mesoporous rhodium film for enhanced nitrogen electroreduction, Nanoscale 13 (32) (2021) 13809–13815, http://dx.doi.org/10. 1039/d1nr03074d.
- [100] Z. Wang, W. Tian, Z. Dai, T. Zhou, Q. Mao, Y. Xu, X. Li, L. Wang, H. Wang, Bimetallic mesoporous RhRu film for electrocatalytic nitrogen reduction to ammonia, Inorg. Chem. Front. 8 (18) (2021) 4276–4281, http://dx.doi.org/ 10.1039/D101007701.
- [101] X. Wang, D. Wu, S. Liu, J. Zhang, X.-Z. Fu, J.-L. Luo, Folic acid self-assembly enabling manganese single-atom electrocatalyst for selective nitrogen reduction to ammonia, Nano-Micro Lett. 13 (1) (2021) 125, http://dx.doi.org/10.1007/ s40820-021-00651-1
- [102] C. Wang, M. Yang, X. Wang, H. Ma, Y. Tian, H. Pang, L. Tan, K. Gao, Hierarchical Co52/MoS2 flower-like heterostructured arrays derived from polyoxometalates for efficient electrocatalytic nitrogen reduction under ambient conditions, J. Colloid Interface Sci. 609 (2022) 815–824, http://dx.doi.org/10. 1016/j.jcis.2021.11.087.
- [103] J. Wang, Z. Jiang, G. Peng, E. Hoenig, G. Yan, M. Wang, Y. Liu, X. Du, C. Liu, Surface valence state effect of MoO2+x on electrochemical nitrogen reduction, Adv. Sci. 9 (12) (2022) e2104857, http://dx.doi.org/10.1002/advs.202104857.
- [104] X. Wei, D. Vogel, L. Keller, S. Kriescher, M. Wessling, Microtubular gas diffusion electrode based on ruthenium-carbon nanotubes for ambient electrochemical nitrogen reduction to ammonia, ChemElectroChem 7 (22) (2020) 4679–4684, http://dx.doi.org/10.1002/celc.202001370.
- [105] X. Wei, M. Pu, Y. Jin, M. Wessling, Efficient electrocatalytic N2 reduction on three-phase interface coupled in a three-compartment flow reactor for the ambient NH3 synthesis, ACS Appl. Mater. Interfaces 13 (18) (2021) 21411–21425, http://dx.doi.org/10.1021/acsami.1c03698.
- [106] J. Xia, H. Guo, G. Yu, Q. Chen, Y. Liu, Q. Liu, Y. Luo, T. Li, E. Traversa, 2D vanadium carbide (mxene) for electrochemical synthesis of ammonia under ambient conditions, Catal. Lett. 151 (12) (2021) 3516–3522, http://dx.doi.org/ 10.1007/s10562-021-03589-6.
- [107] C. Yang, B. Huang, S. Bai, Y. Feng, Q. Shao, X. Huang, A generalized surface chalcogenation strategy for boosting the electrochemical N2 fixation of metal nanocrystals, Adv. Mater. (Deerfield Beach Fla.) 32 (24) (2020) e2001267, http://dx.doi.org/10.1002/adma.202001267.
- [108] H. Yang, Y. Liu, Y. Luo, S. Lu, B. Su, J. Ma, Achieving high activity and selectivity of nitrogen reduction via Fe-N3 coordination on iron single-atom electrocatalysts at ambient conditions, ACS Sustain. Chem. Eng. 8 (34) (2020) 12809–12816, http://dx.doi.org/10.1021/acssuschemeng.0c02701.
- [109] L. Yang, C. Choi, S. Hong, Z. Liu, Z. Zhao, M. Yang, H. Shen, A.W. Robertson, H. Zhang, T.W.B. Lo, Y. Jung, Z. Sun, Single yttrium sites on carbon-coated TiO2 for efficient electrocatalytic N2 reduction, Chem. Commun. 56 (74) (2020) 10910–10913, http://dx.doi.org/10.1039/d0cc01136c.
- [110] X. Yang, S. Sun, L. Meng, K. Li, S. Mukherjee, X. Chen, J. Lv, S. Liang, H.-Y. Zang, L.-K. Yan, G. Wu, Molecular single iron site catalysts for electrochemical nitrogen fixation under ambient conditions, Appl. Catal. B: Environ. 285 (2021) 119794, http://dx.doi.org/10.1016/j.apcatb.2020.119794.
- [111] C. Yao, N. Guo, S. Xi, C.-Q. Xu, W. Liu, X. Zhao, J. Li, H. Fang, J. Su, Z. Chen, H. Yan, Z. Qiu, P. Lyu, C. Chen, H. Xu, X. Peng, X. Li, B. Liu, C. Su, S.J. Pennycook, C.-J. Sun, J. Li, C. Zhang, Y. Du, J. Lu, Atomically-precise dopant-controlled single cluster catalysis for electrochemical nitrogen reduction, Nat. Commun. 11 (1) (2020) 4389, http://dx.doi.org/10.1038/s41467-020-18080-w.
- [112] M. Yuan, H. Zhang, D. Gao, H. He, Y. Sun, P. Lu, S. Dipazir, Q. Li, L. Zhou, S. Li, Z. Liu, J. Yang, Y. Xie, H. Zhao, G. Zhang, Support effect boosting the electrocatalytic N2 reduction activity of Ni2P/N,P-codoped carbon nanosheet hybrids, J. Mater. Chem. A 8 (5) (2020) 2691–2700, http://dx.doi.org/10.1039/C9TA09920D.
- [113] L. Zhang, M. Cong, X. Ding, Y. Jin, F. Xu, Y. Wang, L. Chen, L. Zhang, A janus Fe-SnO2 catalyst that enables bifunctional electrochemical nitrogen fixation, Angew. Chem. (Int. Ed. English) 59 (27) (2020) 10888–10893, http: //dx.doi.org/10.1002/anie.202003518.

- [114] S. Zhang, Q. Jiang, T. Shi, Q. Sun, Y. Ye, Y. Lin, L.R. Zheng, G. Wang, C. Liang, H. Zhang, H. Zhao, Laser irradiation in liquid to release cobalt single-atom sites for efficient electrocatalytic N2 reduction, ACS Appl. Energy Mater. 3 (7) (2020) 6079–6086, http://dx.doi.org/10.1021/acsaem.0c00931.
- [115] S. Zhang, M. Jin, T. Shi, M. Han, Q. Sun, Y. Lin, Z. Ding, L.R. Zheng, G. Wang, Y. Zhang, H. Zhang, H. Zhao, Electrocatalytically active Fe-(O-C2)4 single-atom sites for efficient reduction of nitrogen to ammonia, Angew. Chem. (Int. Ed. English) 59 (32) (2020) 13423–13429, http://dx.doi.org/10.1002/anie. 202005930.
- [116] J. Zhang, B. Zhao, W. Liang, G. Zhou, Z. Liang, Y. Wang, J. Qu, Y. Sun, L. Jiang, Three-phase electrolysis by gold nanoparticle on hydrophobic interface for enhanced electrochemical nitrogen reduction reaction, Adv. Sci. 7 (22) (2020) 2002630, http://dx.doi.org/10.1002/advs.202002630.
- [117] N. Zhang, L. Li, J. Wang, Z. Hu, Q. Shao, X. Xiao, X. Huang, Surface-regulated rhodium-antimony nanorods for nitrogen fixation, Angew. Chem. 132 (21) (2020) 8143–8148, http://dx.doi.org/10.1002/ange.201915747.
- [118] S. Zhang, M. Han, T. Shi, H. Zhang, Y. Lin, X. Zheng, L.R. Zheng, H. Zhou, C. Chen, Y. Zhang, G. Wang, H. Yin, H. Zhao, Atomically dispersed bimetallic Fe-Co electrocatalysts for green production of ammonia, Nat. Sustain. 6 (2) (2022) 169–179, http://dx.doi.org/10.1038/s41893-022-00993-7.
- [119] S. Zhang, T. Shi, K. Li, Q. Sun, Y. Lin, L.R. Zheng, G. Wang, Y. Zhang, H. Yin, H. Zhang, Ambient electrochemical nitrogen fixation over a bifunctional Mo-(O-C2)4 site catalyst, J. Phys. Chem. C 126 (2) (2022) 965–973, http://dx.doi.org/10.1021/acs.jpcc.1c10039.
- [120] S. Zhao, H.-X. Liu, Y. Qiu, S.-Q. Liu, J.-X. Diao, C.-R. Chang, R. Si, X.-H. Guo, An oxygen vacancy-rich two-dimensional Au/TiO2 hybrid for synergistically enhanced electrochemical N2 activation and reduction, J. Mater. Chem. A 8 (14) (2020) 6586–6596, http://dx.doi.org/10.1039/D0TA00658K.

- [121] X. Zhao, Z. Yang, A.V. Kuklin, G.V. Baryshnikov, H. Ågren, X. Zhou, H. Zhang, Efficient ambient electrocatalytic ammonia synthesis by nanogold triggered via boron clusters combined with carbon nanotubes, ACS Appl. Mater. Interfaces 12 (38) (2020) 42821–42831, http://dx.doi.org/10.1021/acsami.0c11487.
- [122] Z. Zhao, Y. Long, S. Luo, Y. Luo, M. Chen, J. Ma, Metal-Free C3N4 with plentiful nitrogen vacancy and increased specific surface area for electrocatalytic nitrogen reduction, J. Energy Chem. 60 (2021) 546–555, http://dx.doi.org/10.1016/j.jechem.2021.01.015.
- [123] L. Zhao, B. Chang, T. Dong, H. Yuan, Y. Li, Z. Tang, Z. Liu, H. Liu, X. Zhang, W. Zhou, Laser synthesis of amorphous CoSx nanospheres for efficient hydrogen evolution and nitrogen reduction reactions, J. Mater. Chem. A 10 (37) (2022) 20071–20079, http://dx.doi.org/10.1039/D2TA01982E.
- [124] J. Zheng, S. Wu, L. Lu, C. Huang, P.-L. Ho, A. Kirkland, T. Sudmeier, R. Arrigo, D. Gianolio, S.C. Edman Tsang, Structural insight into Fe-S2-Mo motif in electrochemical reduction of N2 over Fe1-supported molecular MoS2, Chem. Sci. 12 (2) (2020) 688–695, http://dx.doi.org/10.1039/d0sc04575f.
- [125] Y. Zheng, S. Zhang, H. Yao, X. Li, Y. Su, X. Guo, A-site substitution motivating the phase transformation of LaNiO3 perovskite for high-performance artificial N2 fixation, ChemCatChem 14 (20) (2022) e202200920, http://dx.doi.org/10. 1002/cctc.202200920.
- [126] T. Adachi, Production of high-purity hydrogen through ammonia decomposition and gas removal, in: K.-i. Aika, H. Kobayashi (Eds.), CO2 Free Ammonia As an Energy Carrier, Springer Nature Singapore, Singapore, 2023, pp. 391–400, http://dx.doi.org/10.1007/978-981-19-4767-4\_25.
- [127] K.E. Lamb, M.D. Dolan, D.F. Kennedy, Ammonia for hydrogen storage; A review of catalytic ammonia decomposition and hydrogen separation and purification, Int. J. Hydrog. Energy 44 (7) (2019) 3580–3593, http://dx.doi.org/10.1016/j. ijhydene.2018.12.024, URL https://www.sciencedirect.com/science/article/pii/ S0360319918339272.